NAA-SR-MEMO-8679
COPY 1 2 1 OF 200
93 PAGES
SERIES A

SNAP 10A REACTOR
DESIGN SUMMARY
(Title Unclassified)

ATOMICS INTERNATIONAL
A DIVISION OF NORTH AMERICAN AVIATION, INC.

DISCLAIMER

NAA–SR–MEMOs are working papers and may be expanded, modified, or withdrawn at any time, and are intended for internal use only.

~~SECRET~~

UNCLASSIFIED

NAA-SR-MEMO-8679

~~OFFICIAL USE ONLY~~

SNAP 10A REACTOR

DESIGN SUMMARY

(Title Unclassified)

Edited by

J. SUSNIR
T. HARMAN

~~RESTRICTED DATA~~

ATOMICS INTERNATIONAL

A DIVISION OF NORTH AMERICAN AVIATION, INC.
P.O. BOX 309 CANOGA PARK, CALIFORNIA

CONTRACT: AT(11-1)-GEN-8
ISSUED: DECEMBER 5, 1963

UNCLASSIFIED

~~SECRET~~

BLANK

CONTENTS

CONTENTS

TABLES

TABLES

FIGURES

FIGURES

ABSTRACT

A description of the SNAP 10A reactor subsystem is presented. Design details of the principal assemblies which constitute the reactor subsystem are discussed. System behavior for abnormal conditions such as disassembly during reentry, operation in rain-filled craters, and long-term operation in space are included.

BLANK

I. INTRODUCTION

The SNAP 10A reactor is intended for use as a primary power source on satellites and other space vehicles. Generation of power in space requires a compact system with remote control capabilities, long life, high reliability, and an ability to operate in a space environment characterized by a high vacuum, meteoroid showers and other phenomena not common to terrestrial environments.

The core of the SNAP 10A reactor consists of hydrided zirconium fuel elements enriched with U^{235}. The fuel elements are hydrided to an N_H of 6.35 (6.35×10^{22} atom/cc) which is slightly less than the hydrogen concentration in cold water. The fuel elements are positioned and constrained in the core by upper and lower grid plates. The grid plates are supported by a fixed ring at the bottom and hold-down springs at the top. Beryllium side reflectors are used in the void between the hexagonal fuel element array and the circular reactor vessel. The reactor vessel top head acts both as a vessel closure and restraining structure for the core hold-down springs. The reactor vessel is surrounded by a beryllium structure which functions as the reflector. Four control drums, which form a part of the reflector assembly, provide both the fine and coarse control required for SNAP 10A reactor operation. The lithium hydride shield is positioned directly below the reactor vessel and is contained in a stainless steel casing. A flexible mount is provided to support the LiH within the casing allowing for prelaunch thermal cycling of the system. Control devices such as electric motors, springs, and sensors are attached directly to the reflector assembly. Controlling elements such as timers and reactor controller are located in the instrument compartment.

As described above, the SNAP 10A reactor subsystem (Figure 1) consists of five major subassemblies: the reactor structure, radiation shield, reflector assembly, reactor control equipment and reactor core. Each major subassembly consists of the following components:

A. REACTOR STRUCTURE

1) Reactor vessel
2) Reactor vessel top head
3) Grid plate support ring
4) Reactor vessel support structure

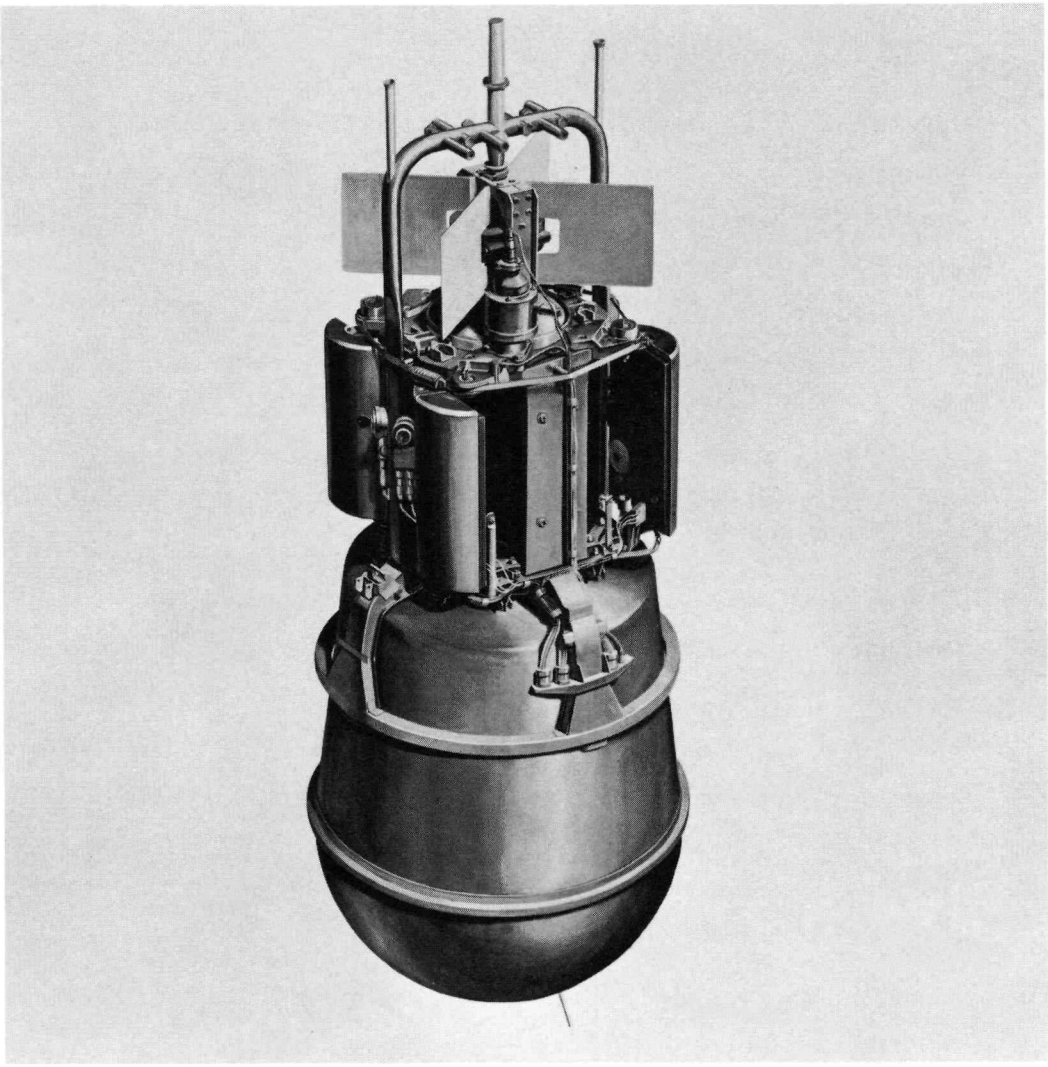

8-1-63 7623-0017

Figure 1. SNAP 10A Reactor and Shield

5) Attachment brackets for pumps, reflectors, etc.
6) Ground safety equipment (shipping sleeve)

B. RADIATION SHIELD

1) Shield casing
2) Shielding material
3) Shield support assembly

C. REFLECTOR ASSEMBLY

1) Main reflector block
2) Control drums
3) Drum drives (gears, bearings, etc.)
4) Actuator motors
5) Position indicators
6) Reflector ejection system (retaining band, springs, actuating devices, etc.)
7) Wiring harness
8) Sensors
9) Ground safety system (void filler blocks)

D. REACTOR CONTROL EQUIPMENT

1) Controller
2) Timer
3) Temperature sensor switches

E. REACTOR CORE

1) Grid plates
2) Fuel elements
3) Core positioning mechanism
4) Internal reflectors

Basic design parameters for the SNAP 10A reactor subsystem are given in Table I. Table II gives the shock and vibration environment which components and subassemblies have been designed to withstand.

TABLE I

SNAP 10A REACTOR DESIGN SUMMARY

Operating Conditions	
Reactor thermal power (kwt) - Average	34
Net electrical power (watt) - Minimum	500
Operating life	1 yr
NaK outlet temperature (°F) Control Point	1010
NaK inlet temperature (°F)	900
NaK operating pressure (psia)	10
Maximum fuel temperature (°F)	1085
Maximum cladding temperature (°F)	1050
Reactor Design	
Fuel elements	
Number	37
Fuel alloy (wt% U in Zr)	10
Degree of hydriding N_H (10^{22} atom/cm^3)	6.35
Cladding material	Hastelloy-N
Fuel diameter (in.)	1.212
Cladding diameter (OD, in.)	1.25
Cladding thickness (in.)	0.015
Active fuel length (in.)	12.25
Internal reflectors	
Material	Be
Cladding	None
Inlet plenum grid plate (lower)	
Material	Hastelloy-C
Thickness (in.)	1/2 (sandwich construction)
Outlet plenum grid plate (upper)	
Material	Hastelloy-C
Thickness (in.)	1/8
Core Vessel	
Material	316 SS
Internal diameter (in.)	8.875
Length (in.)	15.6
Wall thickness (in.)	0.032

TABLE I (Continued)

SNAP 10A REACTOR DESIGN SUMMARY

Reflector control elements	
Number	4
Material	Be
Nominal thickness (in.)	2
Nuclear Parameters	
Average core thermal flux (n/cm^2-sec)	1.9×10^{11}
Mean fission energy (ev)	0.18
Average isothermal temperature coefficient (¢/°F)	-0.22
Uranium loading (kg U^{235})	4.75
Effective delayed neutron fraction	0.008
Mean prompt neutron lifetime (μ-sec)	6.5
Burnable poison	
Material	Sm_2O_3
Prepoison reactivity worth ($)*	-1.80
Initial cold excess reactivity ($)*	2.62
Total lifetime reactivity loss ($)*	-2.24
Xenon equilibrium	-0.12
Samarium burnout	+0.17
Temperature and power defect	-2.04
Hydrogen loss	-0.06
Hydrogen redistribution	-0.13
Burnup and fission product poisons	-0.06
Contingency	+0.38
Total control drum worth ($)*	8.80
Total shim capability ($)*	1.26
Shield Parameters	
Material	LiH
Dimensions	
Maximum diameter (in.)	21.08
Minimum diameter (in.)	17.56
Height (in.)	27.47

*one dollar = 0.008 Δ k/k

TABLE I (Continued)

SNAP 10A REACTOR DESIGN SUMMARY

Shield casing	
Material	316 SS
Thickness (in.)	0.032
Integrated radiation doses below shield for 1 year of full power operation (fast neutrons and gammas)	
Mating plane (NPU-Booster)	
Center of plane r = o	1.5×10^{12} nvt 6.2×10^{6} r
Inner edge of instrumentation compartment (max) (r = 13-3/4 in.)	4.5×10^{12} nvt 8.5×10^{6} r
Outer edge of instrumentation compartment (max) (r = 24-1/2 in.)	2.0×10^{14} nvt 9.2×10^{6} r
Reference plane (17-1/2 ft below core)	
Center of plane r = o	4.5×10^{11} nvt 1.5×10^{6} r
Outer edge of plane (max) (r = 30 in.)	1.9×10^{13} nvt 2.0×10^{6} r
Weight Summary	
Reactor, core and vessel assembly (lb)	168
Reflector-control assembly (lb)	106
Shield assembly (lb)	217
Electronic equipment (lb)	13
Total nuclear system (lb)	504

TABLE II

SHOCK AND VIBRATION ENVIRONMENT PARAMETERS OF SNAP 10A REACTOR SUBSYSTEM TESTS

	Shock				Vibration		
	Shape	Axes	Magnitude (g)	Duration (μ sec)	Axes	Magnitude (g)	Frequency (cps)
Assemblies	Half sine wave	Longitudinal	5.5	8	Longitudinal	0.5 in. DA	5 to 12
						3.5	12 to 400
		Lateral and Normal	1.5			7.5	400 to 3000
					Lateral and Normal	0.5 in. DA	5 to 10
						2.5	10 to 250
						5	250 to 400
						7.5	400 to 3000
Components	Half sine wave	Longitudinal	20	6	Longitudinal	1/4 in. DA	5 to 30
						12*	30 to 250
		Lateral and Normal	10			5	250 to 400
						7.5	400 to 3000
					Lateral and Normal	1/4 in. DA	5 to 20
						5	20 to 400
						7.5	400 to 3000

*Instrument compartment components only. Other reactor subsystem components are required to withstand 5g over this frequency range

BLANK

II. REACTOR STRUCTURE AND CORE

The SNAP 10A reactor structure has been designed to support the reactor core, reflectors, and NaK coolant pump, and to contain the NaK during prelaunch checkout, launch, and orbital operating conditions. Structural behavior under a variety of environmental conditions was considered in establishing the final configuration. Environmental conditions studied are listed below.

a) Accelerations during launch

b) Coolant system pressure

c) Space vacuum

d) Corrosion by NaK

e) Elevated temperature

f) Neutron flux

The reactor structure and core consists of a reactor vessel assembly, 1 top head, 2 grid plates, 6 internal reflectors, 12 hold-down springs, 37 fuel elements, and 4 support legs. The reactor core and vessel (including grid plates) weighs 168 lb. Approximately 7 lb of this is NaK coolant.

The reactor vessel assembly shown in Figure 2 consists of a deep drawn and spun reactor vessel to which a support ring, 2 NaK inlet pipes, and reflector support bracketry are welded. The assembly is constructed entirely of stainless steel, Type 316. The reactor vessel has an inside diameter of 8.875 in. and an overall length of approximately 16 in. It is essentially a right circular cylinder with the lower closure an inverted dome. Wall thicknesses vary from 0.032 in. in the core region to 0.125 in. in areas to which attachments are welded. The fuel elements are supported and positioned in the reactor vessel by the 2 grid plates which are shown in Figures 3 and 4. Each plate is 8.750 in. in diameter and is fabricated from Hastelloy C alloy. The upper plate is a solid piece of material 0.125 in. thick. The lower plate is a brazed assembly consisting of a 0.060-in.-thick baffle plate and a 0.060-in.-thick orifice plate with spacers between them. The overall thickness of the lower grid plate is 0.500 in. The plates have 37 holes arranged on a 1.260-in.-triangular pitch for positioning the fuel elements. The plates are also perforated with 72 holes on a 0.728-in.-triangular pitch for coolant flow. The diameter of the flow holes in the upper

BLANK

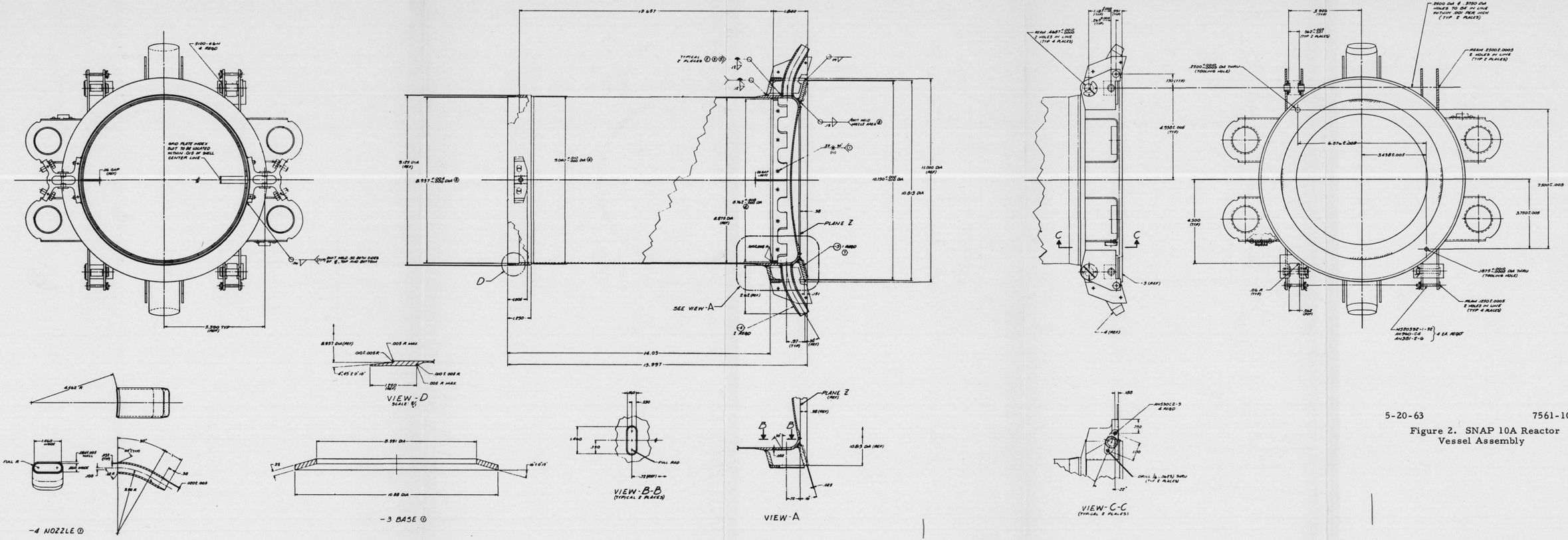

5-20-63 7561-1049

Figure 2. SNAP 10A Reactor Vessel Assembly

BLANK

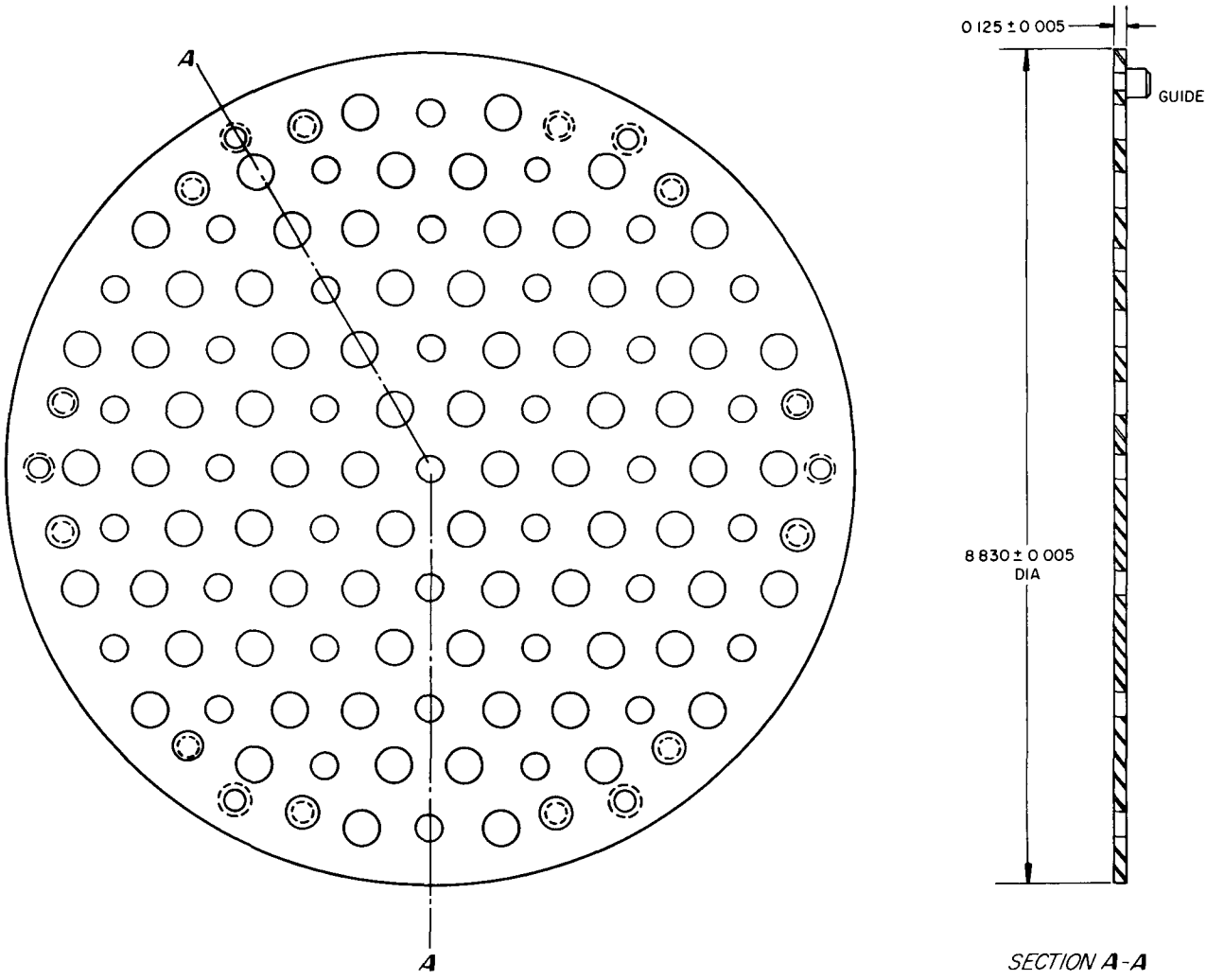

7-15-63

7623-0013

Figure 3. SNAP 10A Upper Grid Plate Design

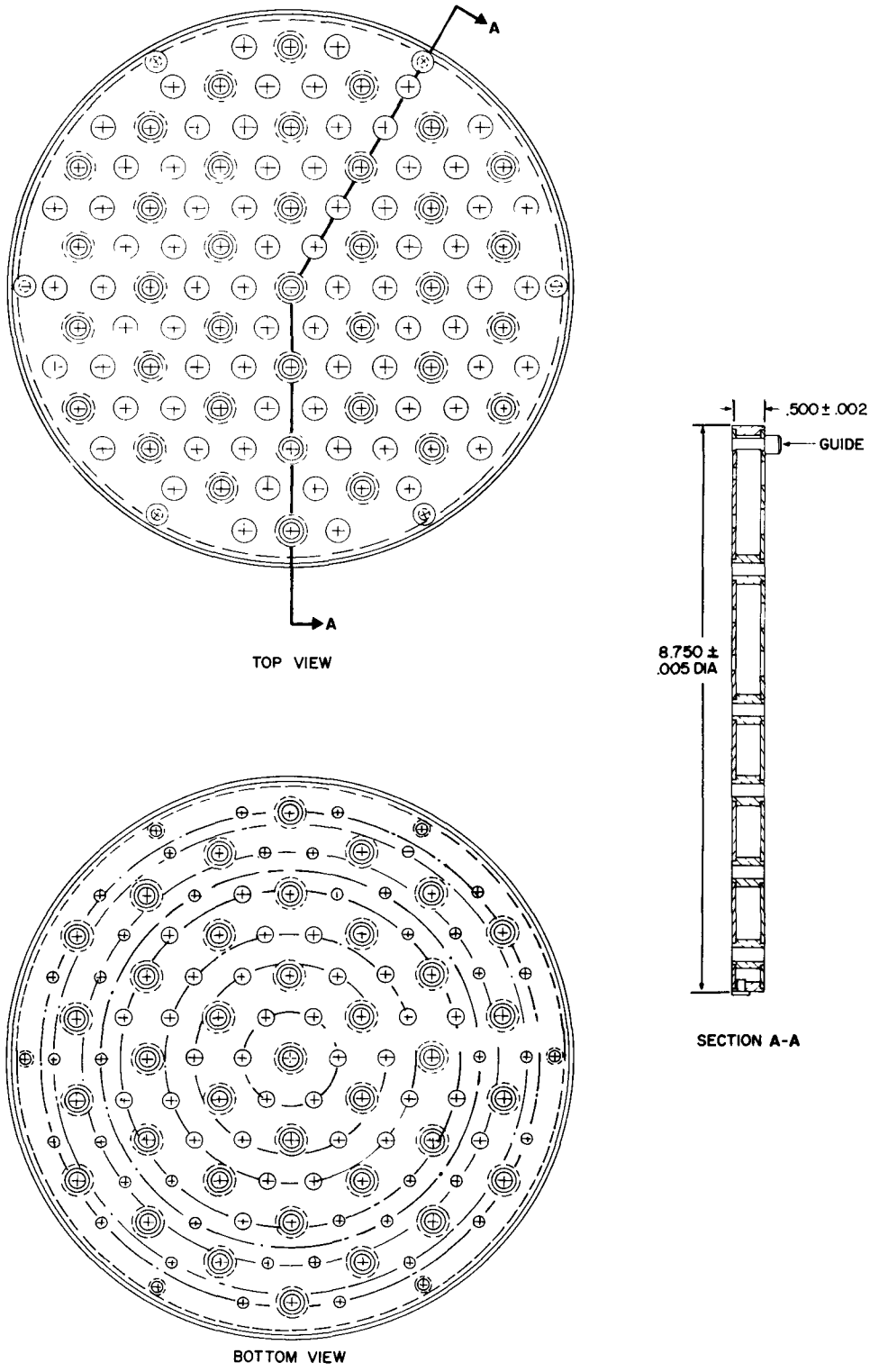

7-15-63 7623-0014

Figure 4. SNAP 10A Lower Grid Plate

grid plate, and the baffle plate of the lower grid plate is 0.375 in. The diameter of the flow holes in the orifice plate varies from 0.250 in., surrounding the central fuel element, to 0.188 in. at the outermost ones. Six pins are attached to each plate for positioning of the internal reflectors. Twelve pins are attached to the upper grid plate for location of the core hold-down springs.

Six beryllium internal side reflectors as shown in Figure 5 are positioned between the grid plates; pins in the grid plates mate with holes in the reflectors. The reflectors are 12.455 in. in length and are shaped to fit fuel element and reactor vessel wall contours. The internal reflectors have no major structural function.

The reactor vessel top head, Figure 6, is the final closure for the reactor vessel. It is forged from stainless steel, Type 316. In finished form, it is a 150° cone with a NaK outlet at the center and a flange at the outer edge for attachment to the reactor vessel. The wall thickness of the conical section is 0.095 in. Sockets are forged in the head for locating the core hold-down springs and also for attachment of the pump support outriggers. The flange has an extended lip which is welded to the reactor vessel. This simplifies the final closure operation and provides a configuration which facilitates top head burnoff during atmospheric reentry.

Twelve core hold-down springs are compressed between the reactor vessel top head and the upper grid plate. These springs hold the core in place during launch operations but allow relative thermal expansion between the core and reactor vessel. The springs are fabricated from Rene 41 wire and exert a force of 37.5 lb each as installed. Free and compressed lengths are 0.605 and 0.500 in., respectively.

The reactor is supported on the converter structure by four support legs (Figure 7) formed from 0.032-in. 4AL-6V titanium alloy and welded. The legs are designed to support the reactor structure, with NaK pump and reflectors attached, during launch. The legs permit relative thermal expansion between the reactor and converter structure. The support legs are attached to both reactor and converter structures with blind bolts.

During launch the reactor structure will experience simultaneous accelerations in both longitudinal and lateral directions. For design calculations, three extreme conditions were considered:

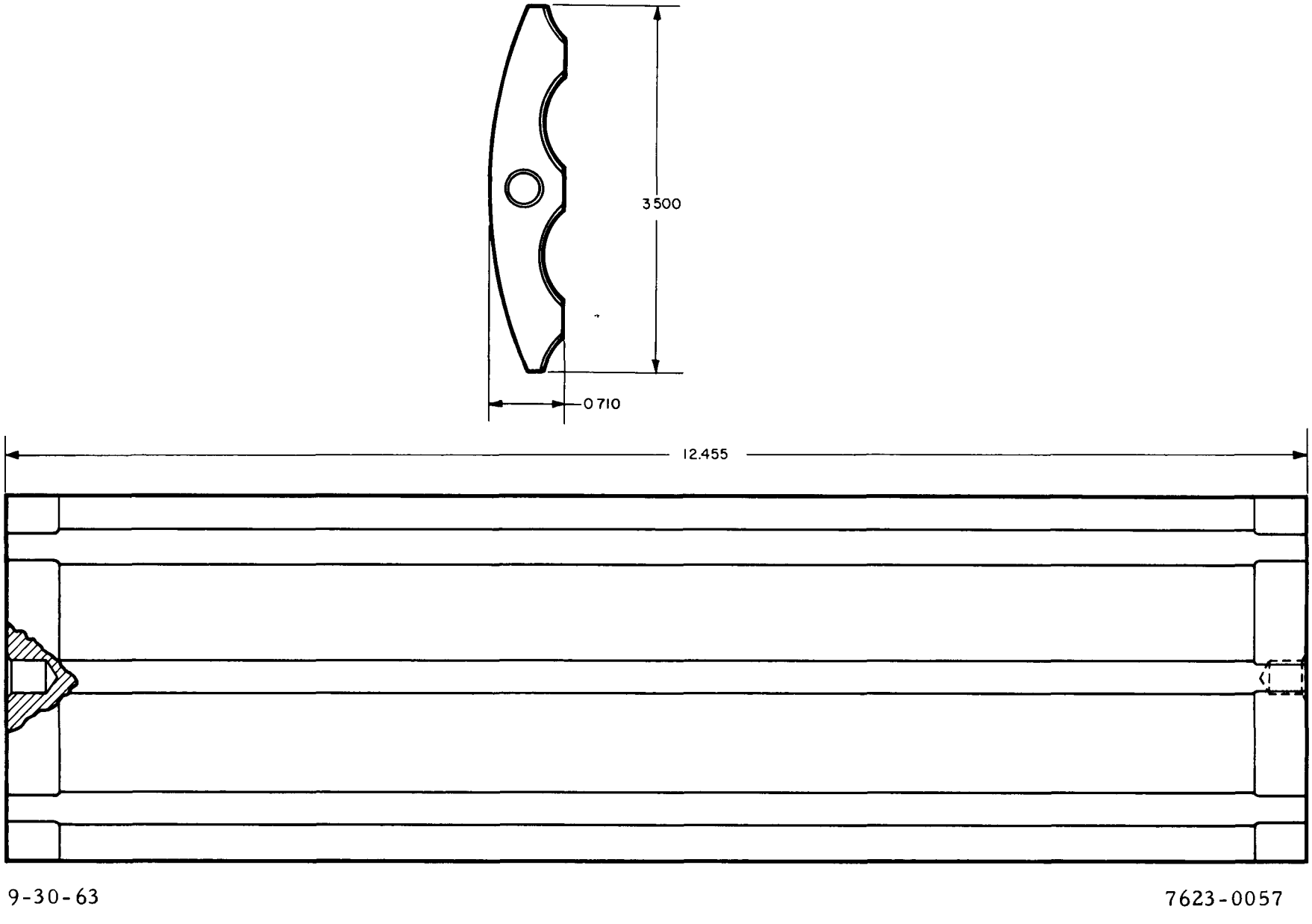

Figure 5. Reactor Vessel Internal Reflectors

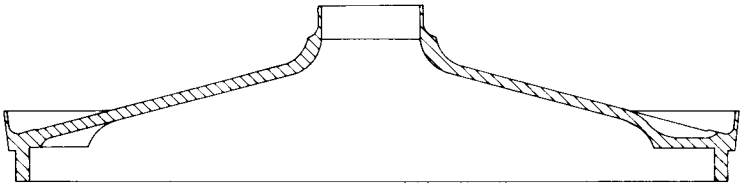

SECTION A-A
BASIC TOP HEAD

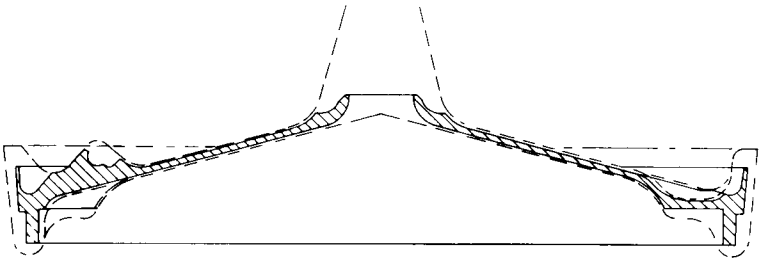

SECTION F-F
-4 TOP HEAD

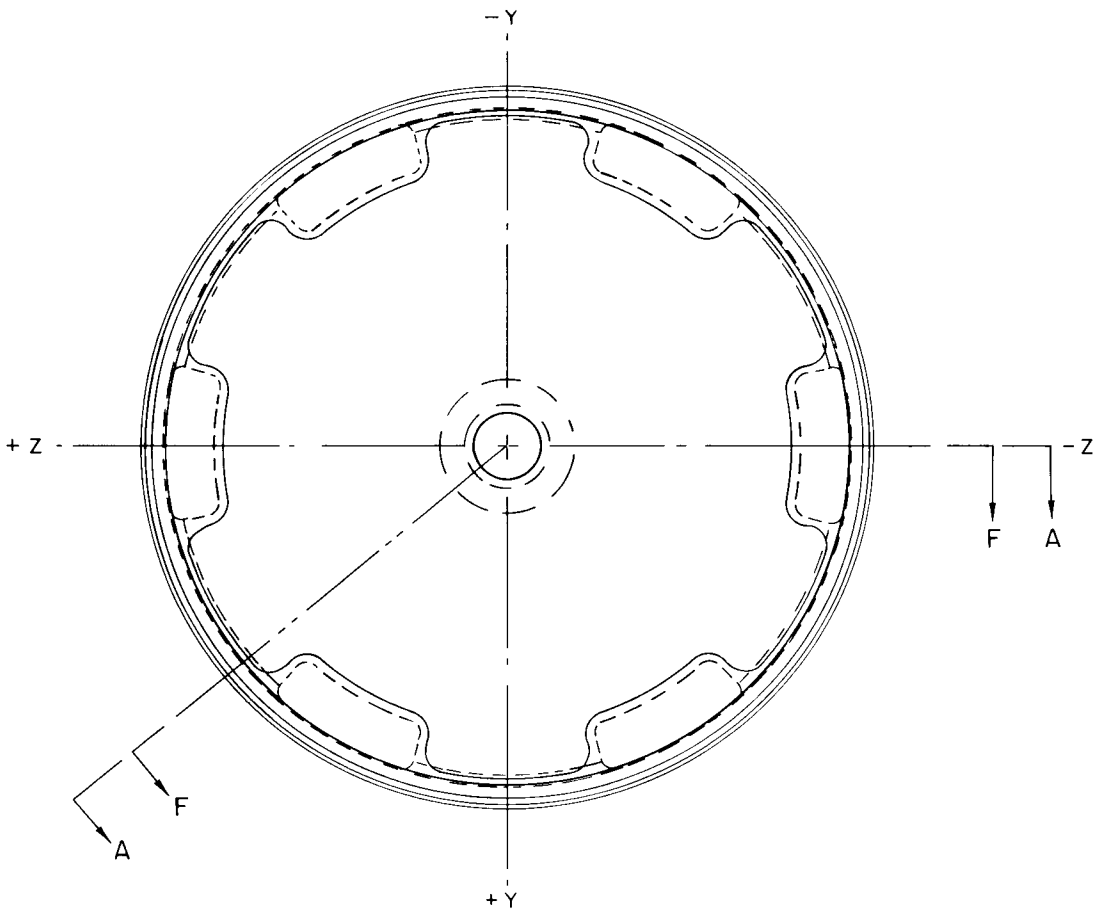

7-15-63

7623-0015

Figure 6. Reactor Vessel Top Head

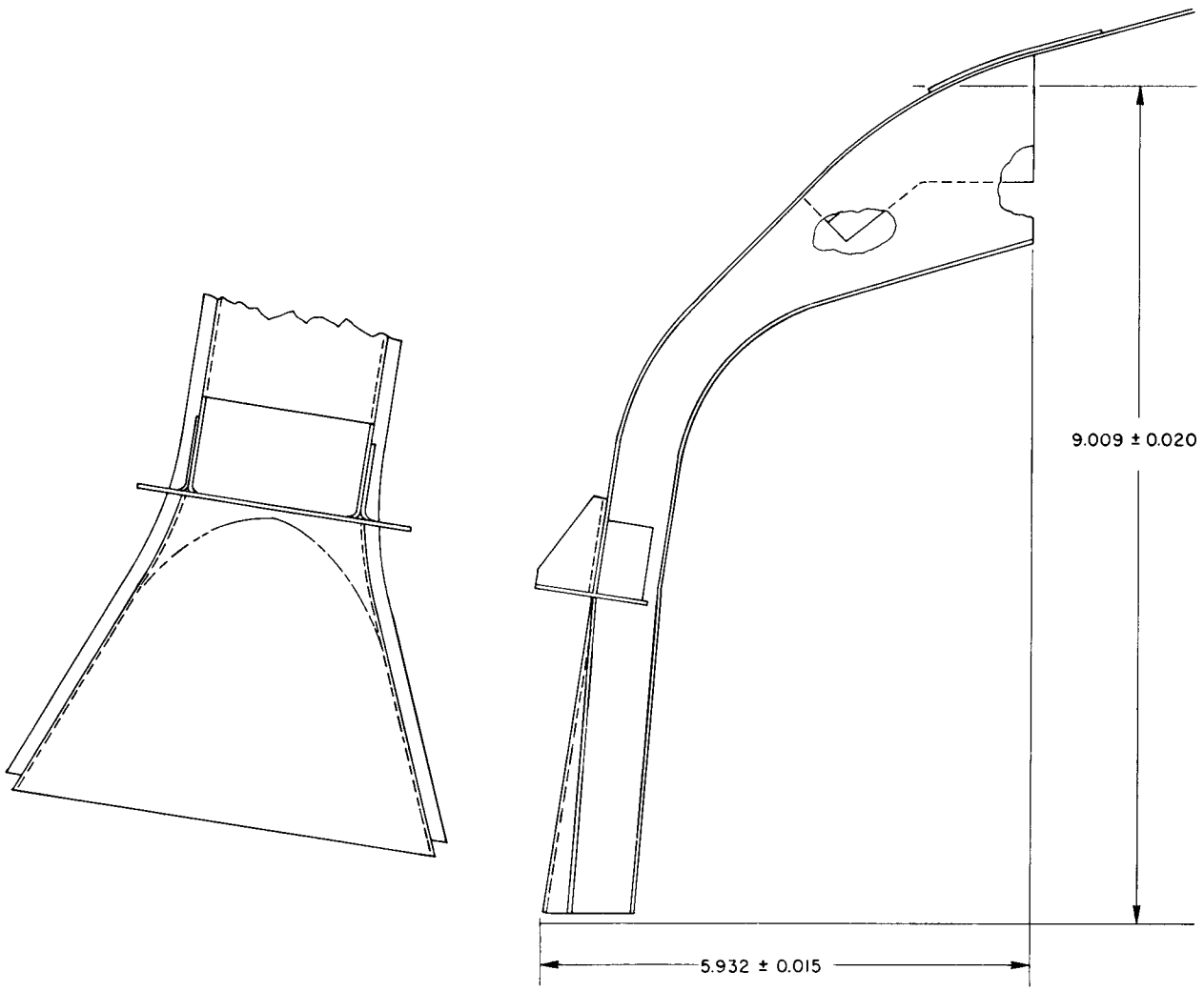

7-15-63

7623-0016

Figure 7. Reactor Support Legs

a) 7.5 g aft	±1.0 g lateral
b) 2.5 g forward	±1.0 g lateral
c) ±2.0 g longitudinal	±5.0 g lateral

Because the reactor structure is cantilevered on the support legs in the lateral direction, condition (c) has proved to be the most severe mode of loading. The most critical area is the "knee" of the support legs. Stresses calculated on the basis of static loading indicate a factor of safety of about four on the ultimate load-carrying capacity. Because of the low ductility of titanium, a fatigue problem is created by stress concentration in welded areas; the safety margin is very much reduced. Experimental studies, however, have confirmed the integrity of the design. Other critical areas include the blind bolt joints between the legs and the vessel and the attachment between the vessel and reflector positioning bracket. Unlike the support legs, local failure in these two cases would not necessarily jeopardize mission success.

During orbital operation, the following nominal conditions will exist for 1 yr:

Average core temperature	$955\ ^{+20\,^\circ F}_{-35\,^\circ F}$
Coolant system pressure	10 psia

Because launch loading and fabricability impose more stringent design requirements on the reactor vessel and top head than does internal pressure, the stresses under this condition are quite nominal. Thermal stresses, even under transient startup conditions, are likewise small. The pressure drop through the entire reactor is 0.17 psi and provides no significant load on the grid plates.

By proper selection of materials, problems created by space vacuum and NaK corrosion have been eliminated. Irradiation damage to the reactor structure during the design lifetime is expected to be negligible since the integrated fast neutron flux is well below the 10^{21} nvt considered to cause problems in austenitic stainless steel. The portions of the reactor exposed to meteoroid bombardment are the top head and the top portion of the vessel where the wall thickness is 0.095 in. For structural reasons, these surfaces are much thicker than required for meteoroid protection.

During handling operations, when the reflector is not attached to the reactor vessel, a shipping sleeve will be installed around the vessel. This device is designed to maintain the reactor subcritical with water in the core and infinite water surrounding the reactor vessel. Figure 8 illustrates the configuration of the shipping sleeve. The sleeve is designed to withstand a free fall of 15 ft onto a concrete surface, retaining its structural integrity. The void space between the inner and outer cylinders of the sleeve are compartmentized to ensure subcriticality if as many as three compartments are filled with water.

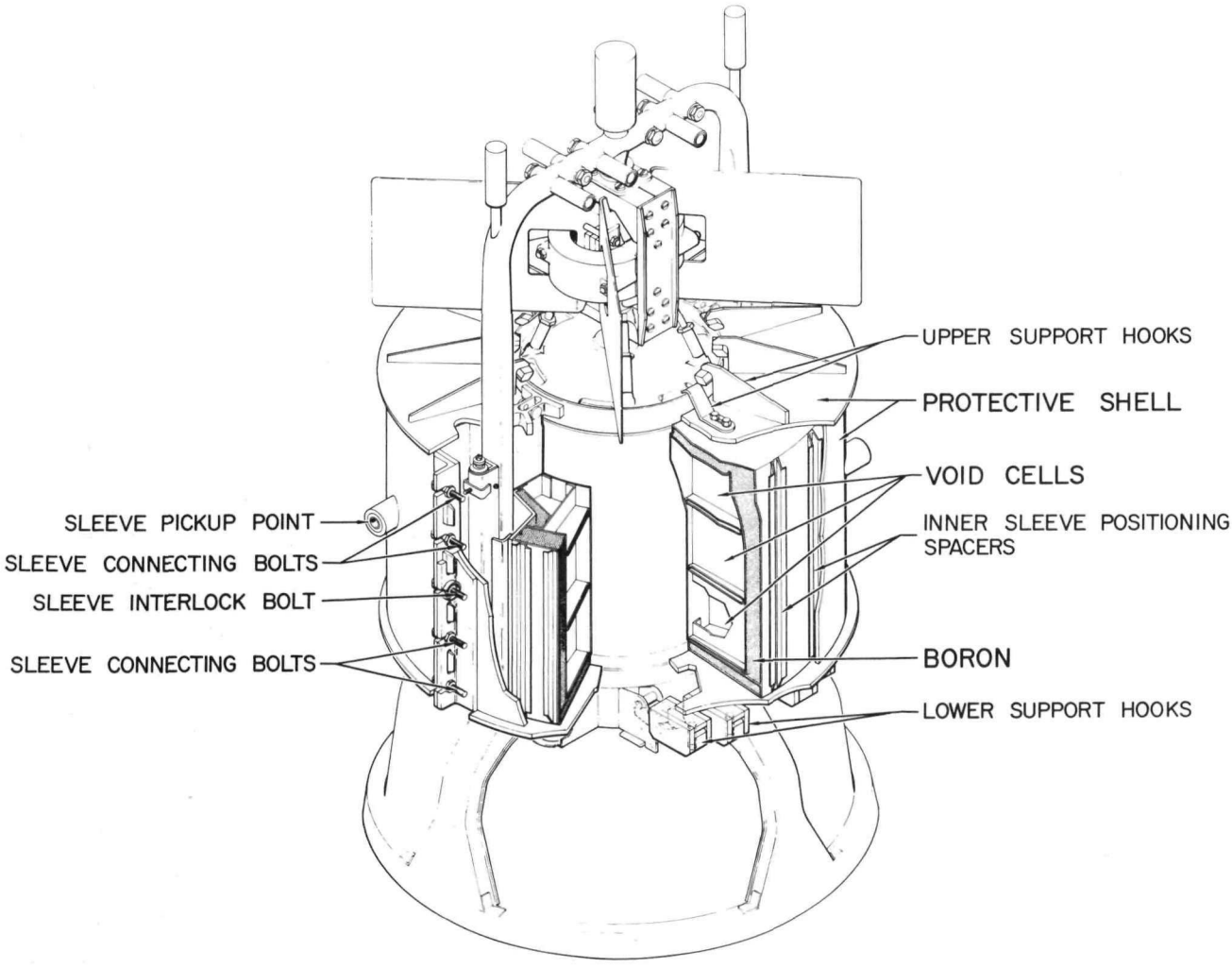

6-27-63

7561-0514

Figure 8. SNAP 10A Shipping Sleeve Assembly

III. RADIATION SHIELD

The SNAP 10A shield is a shadow shield. Its configuration is determined by the outer extremities of the reactor assembly and the 5-ft-diameter dose plane, located 17.5 ft below the bottom of the reactor core. The shield assembly is located directly below the reactor and has a total weight of 217 lb. For normal reactor operation at an average thermal power of 34 kw for 1 yr, the gamma and fast neutron flux levels for neutron energies above 0.1 Mev are described in Table III.

TABLE III

GAMMA AND FAST NEUTRON FLUX LEVELS FOR NORMAL REACTOR OPERATION FOR 1 YR

Plane	Location	Fast Neutrons ($n/cm^2/yr$ at 34 kwt)			Gamma Dose Rate (r/yr at 34 kwt)
		Radius (in.)	Minimum	Maximum*	
Mating	Centerline	0	3.7×10^{12}	3.7×10^{12}	9.6×10^{6}
Mating	Instrument compartment inner edge	13-3/4	2.9×10^{12}	5.2×10^{12}	1.4×10^{7}
Mating	Instrument compartment outer edge	24-1/2	5.5×10^{13}	2.0×10^{14}	1.6×10^{7}
Mating	Outer edge of plane	30	1.6×10^{14}	3.0×10^{14}	1.6×10^{7}
Reference	Centerline	0	9.0×10^{11}	9.0×10^{11}	2.1×10^{6}
Reference	Outer edge of plane	30	6.0×10^{12}	2.6×10^{13}	2.9×10^{6}

*Maximum neutron dose occurs directly below fine control drums.

The SNAP 10A shield assembly utilizes a cold-pressed lithium hydride shielding material reinforced with stainless steel honeycomb and contained in a Type 316 stainless steel casing. The honeycomb matrix is used to eliminate crack propagation and to hold the lithium hydride block together when subjected to thermal gradients. The honeycomb matrix consists of 0.001-in.-thick stainless steel foils which divide the shield into 1-in. square cells. The foil contains 1/2-in. perforations on 3/4-in. centers to permit even distribution of the granular hydride prior to cold-pressing. Experience at the Oak Ridge National Laboratories (ORNL) motivated the selection of the cold-pressed honeycombed compact as the form most resistant to cracking under thermal cycling. Figure 9 is a photograph showing the effects of the honeycomb matrix on a typical SNAP 10A shield configuration which has been subjected to thermal cycling. Cold-pressing with a thick-walled honeycomb matrix results in a lower density shield. The thin, perforated foil presently being utilized offers low resistance to the compacting forces thereby assuring high lithium hydride densities while maintaining sufficient structural integrity of the block.

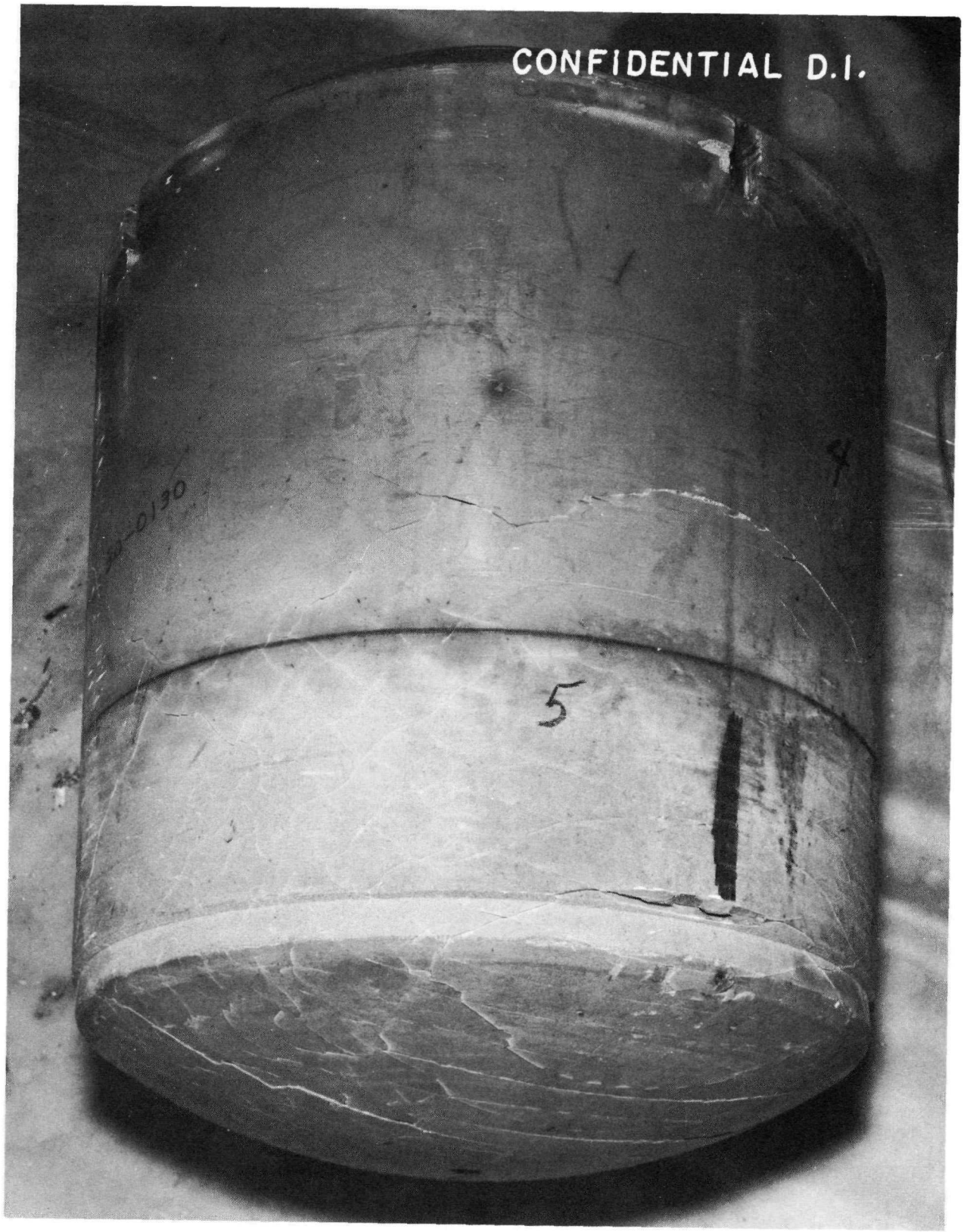

2-28-62

7580-1008

Figure 9. SNAP 10A Shield after Thermal Cycling

The compressive and tensile strengths for cold-pressed LiH at room temperature are 10,000 and 1,500 psi respectively. At elevated temperatures, the allowable material stresses are reduced considerably. At an average operating temperature of 800°F the allowable compressive and tensile stress levels, compared to room temperature values, are reduced by a factor of five. (The melting point of lithium hydride is 1240°F.)

To position the hydride against the forward end of the casing during the launch phase, a spring-supporting mechanism preloads the hydride to an equivalent 7.5 g vertical acceleration load. This is the maximum acceleration force expected during launch. The springs permit expansion of the hydride during prelaunch thermal testing and at operating temperatures. The supporting mechanism consists of eight spring assemblies. The springs are attached to the shield casing and to a parabolic plate below the shield, thus forming a "sling" supporting the shield from below. The support plate was sized in such a manner as to distribute its load uniformly and minimize creep effects in the LiH material. Excessive creep, incurred during prelaunch thermal operation, would cause relaxation of the pretensioning load. Once in orbit, creep of the LiH material has no harmful effect. Below 700°F, LiH will creep less than 1% under a compression load of 350 psi. Above this temperature the creep rate accelerates rapidly resulting in gross deformations. A bearing stress of 28 psi, resulting from the 7.5 g pretensioning load, is present in the vicinity of the parabolic plate. At an average operating temperature of 800°F the lithium hydride expands relative to the casing and induces an additional bearing stress of 25 psi. Thus, the maximum bearing stress on the LiH at operating temperatures is 53 psi.

The pretensioning load from the springs to the hydride is accomplished by eight turnbuckle assemblies. The turnbuckle assembly consists of a threaded eye-bolt which is hooked to the spring, a turnbuckle barrel, and a threaded T-bolt which terminates at a fastening lug brazed to the stainless steel casing. (See Figure 10.) Inconel-X helical coiled springs are utilized to minimize relaxation at temperature. The preload stress in each spring is 59,500 psi. At operating conditions the total maximum stress in the spring caused by both the pretensioning and expansion of the hydride is 89,000 psi at 750°F.

During prelaunch thermal operation, a 3% relaxation occurs in the springs. Relaxation of the springs during long-term temperature operation in orbit is not detrimental; relaxation of the springs reduces the bearing load on the lithium hydride.

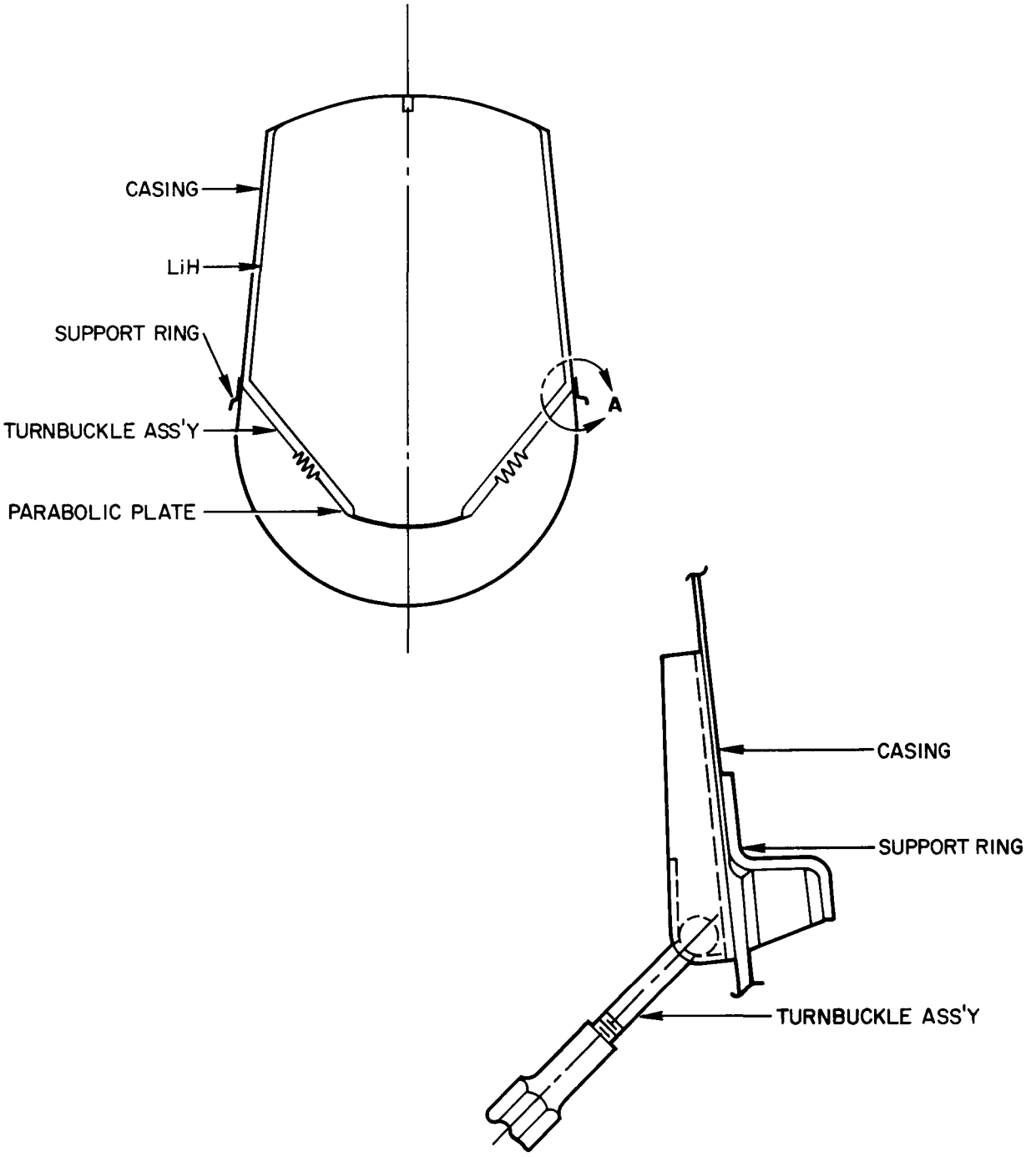

7-10-63

7623-0004

Figure 10. Turnbuckle Assembly

Thickness and size of the shield casing is based on limiting the membrane stresses due to internal pressure to 90% of yield stress at temperature. For a temperature of 800°F the allowable membrane stress of stainless steel 316 is 20,000 psi. At operating conditions, the shield casing is subjected to an internal pressure of 42 psi. The maximum membrane stress due to pressure at an operating temperature of 800°F is 15,400 psi. (At this temperature a pressure of 191 psi would be required to rupture the casing.)

The major contribution of pressure buildup in the shield assembly is the differential expansion between LiH and the stainless steel casing (the coefficient of thermal expansion for lithium hydride is approximately 2-1/2 times that of stainless steel). Lithium hydride expands relative to the casing and compresses the cover gas within the void provided. The casing weight was optimized on the basis of internal pressure and wall thickness, yielding an optimum void volume (Figure 11).

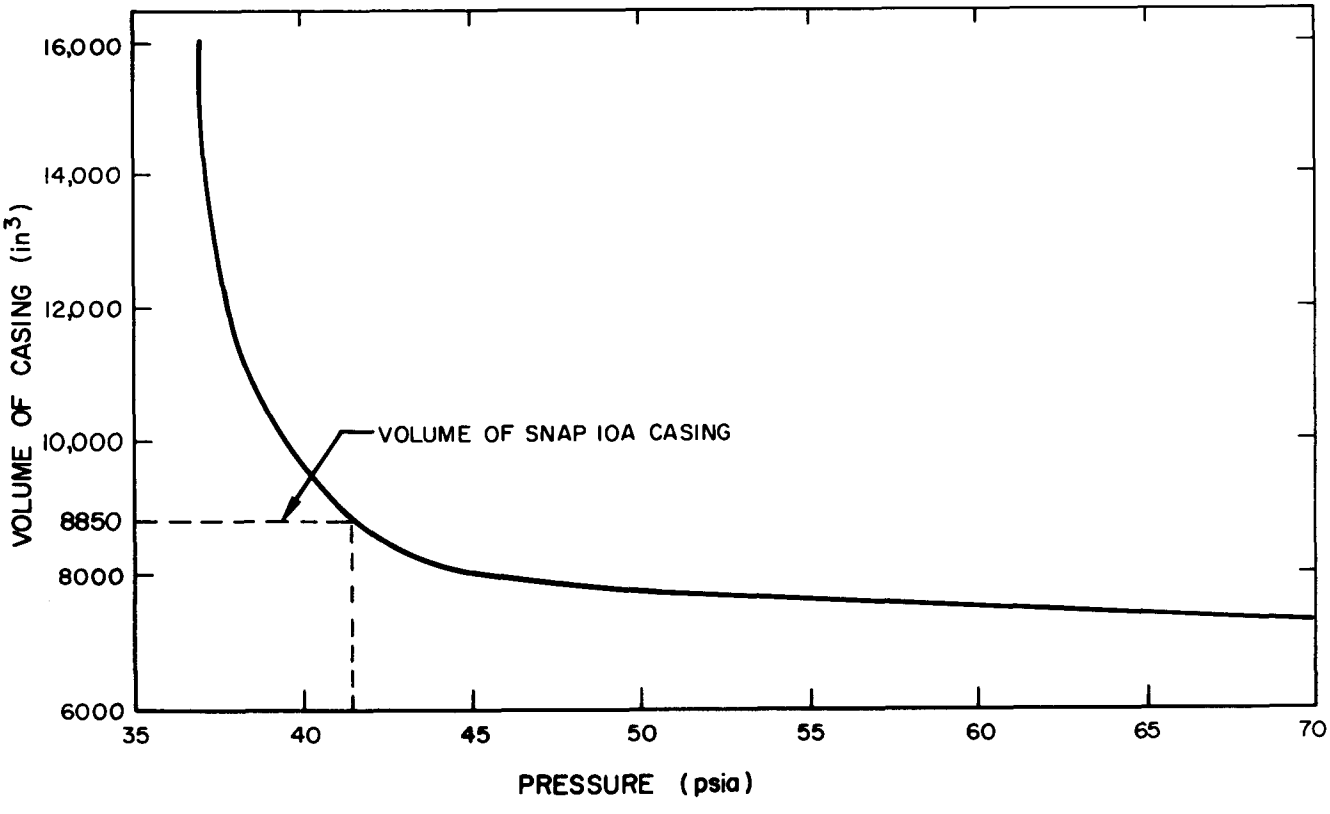

Figure 11. Shield Casing Volume vs Pressure

Each shield received by AI must be certified with respect to an outgassing potential. This is to ensure that lithium hydride shields have been properly handled during fabrication and that pressure buildup resulting from outgassing during a long shelf life of the assembly (approximately 1 yr) is minimized. Certification consists of guaranteeing that the total amount of hydrogen gas which may be evolved during the LiH-H_2O reaction is limited to 0.5 cc of H_2 per square inch of LiH surface area.

During prelaunch and orbital operations, the shield casing will be exposed to the steady-state temperature environment described below.

a) The lower end will see the inside of the support structure which will be at an average temperature of 800°F.

b) The upper surface shall see the base of the reactor vessel at approximately 900°F.

c) The lower side shall be adjacent to the power system converter structure which will be at a temperature of 840°F.

d) The upper side area and part of the upper surface shall be exposed to the space environment.

The reactor shield was designed to be removable from the power system by use of bolted attachments. The shield will withstand the thermal cycling encountered during prelaunch testing in a 1 g environment. The maximum vibratory and static loads encountered at launch are +7.5 g, -2.5 g longitudinal in combination with 1 g lateral, or 5 g lateral in combination with 2 g longitudinal. When these loads are present, the shield temperature should not exceed 100°F. During orbital operation, the shield shall function in a zero g space environment and will be subjected to the thermal environment given above. Transient and steady-state temperatures are given in Figure 12. Temperatures are given for the case of no internal heat generation to correlate nonnuclear testing results.

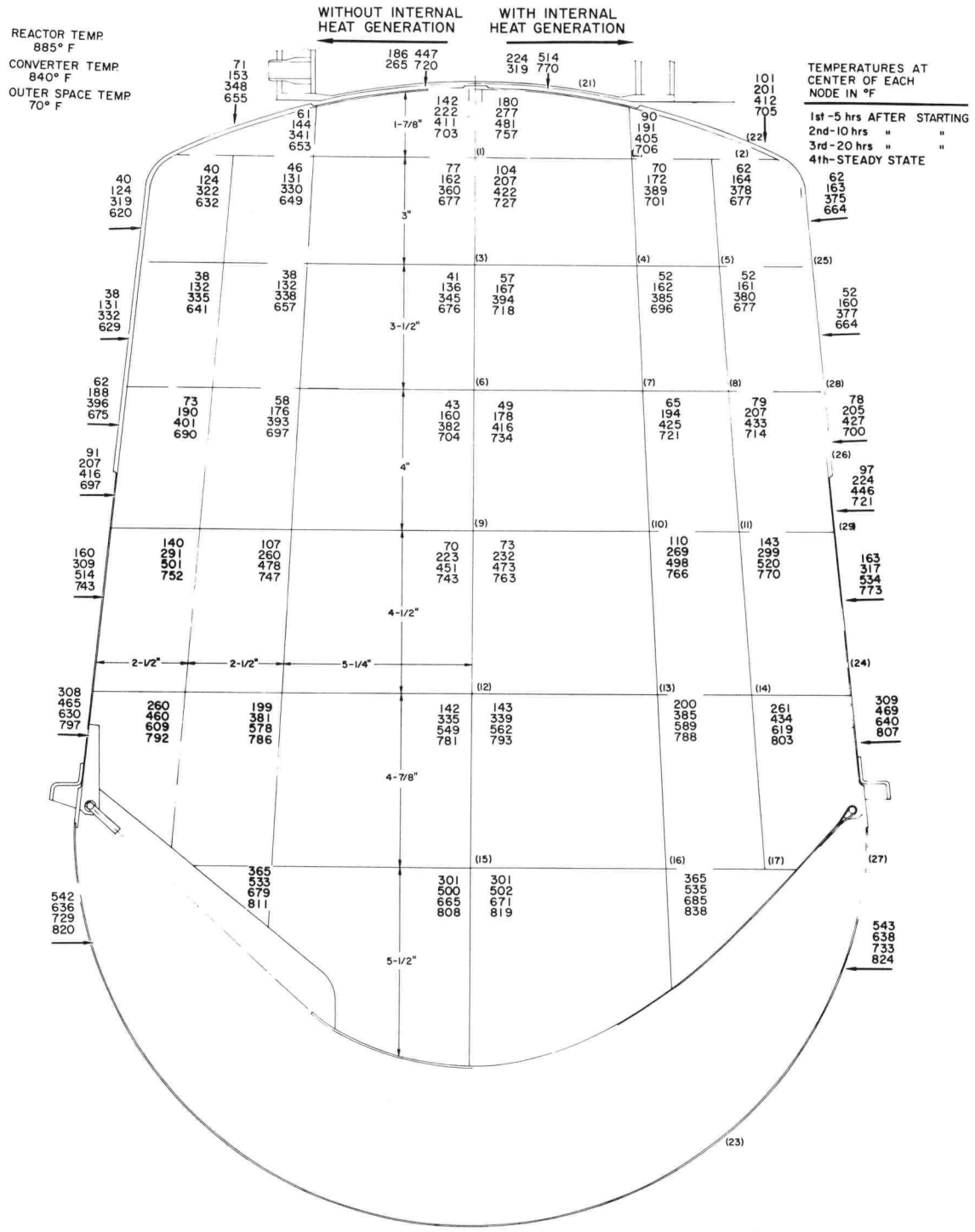

11-21-62

7573-5623D

Figure 12. SNAP 10A Shield Temperatures (LiH in Pressed Form)

BLANK

IV. REFLECTOR AND SAFETY DEVICES

The control and reflector assembly shown in Figure 13 can be divided into four subassemblies which include the safety devices. These subassemblies overlap in many respects, but are sufficiently distinct to explain the various features of the completed assembly. These subassemblies are the reflector and control assembly, support assembly, ejection assembly, and ground safety assembly.

A. REFLECTOR AND CONTROL ASSEMBLY

The reflector consists of a beryllium sleeve, approximately 2 in. thick, surrounding the reactor core. The inside of this sleeve is a cylinder, while the outside is made up of plane sections approximating a cylinder.

Control of reflectivity is obtained by using four drums. In their full in position, these drums complete the reflecting sleeve; however, they may be rotated to a position 135° from the full in position leaving a cavity in the sleeve. Each drum may be increased in thickness with as many as three 1/8-in.-thick shims. With the control drums in their full out position, the reactor is adjusted to be $6.13 subcritical at room temperature.

When the startup command is received, squibs are fired in actuators adjacent to each control drum. This action pulls a pin, releasing the drum. The two coarse control drums are spring-loaded, and when released, are immediately inserted. This adds $4.40 of reactivity. Fifty seconds after the startup command is received, the two fine control drums take their first step. They then move a half-degree step each 150 sec until reactor operating temperature is reached. It will be approximately 7 hr after startup before criticality is reached, and approximately 2 hr more before operating temperature is reached.

The temperature switch located in the outlet NaK line is set for 1010 ± 10°F, and will control the reactor during full power operation. When the outlet temperature drops below the set point, the fine control drums will take another step inward. This continues until 72 hr after the startup command, at which time the control system is commanded "off."

The unique features of the coarse control drum package include the snap-in spring, coarse control drum stop, and the drum release system.

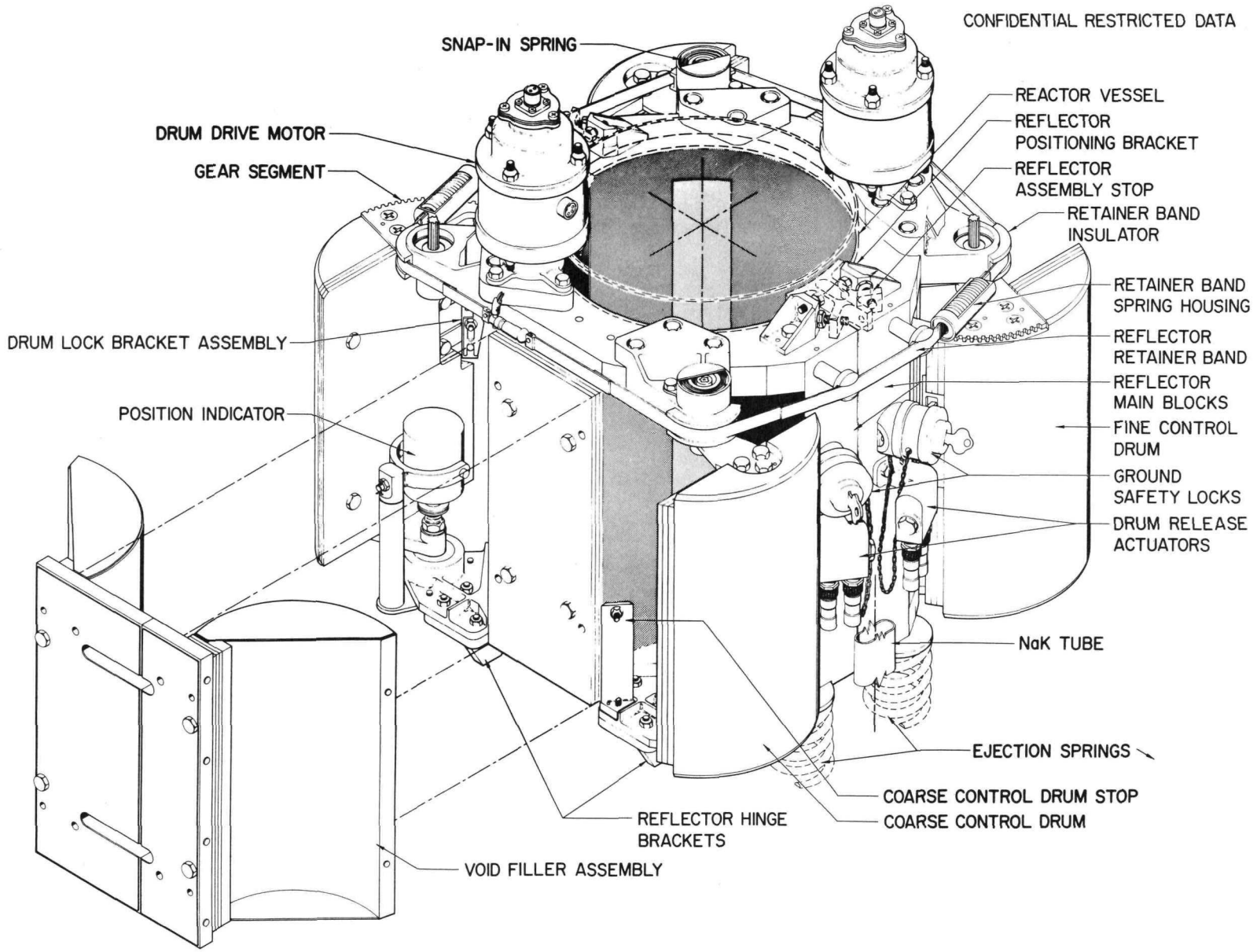

Figure 13. Reactor Reflector Assembly

The snap-in spring is a flat wire torsion spring, made of Rene 41, which exerts a 10-in.-lb moment on the drum shaft in the full out position and a 5-in.-lb moment on the shaft in the full in position. The lower torque provides a factor of safety of approximately two over the maximum expected bearing friction, and guarantees that the drum will stop in the full in position.

The coarse control drum stop is a stiff Rene 41 cantilever spring which stops the drum in the full in position. It has enough flexibility to stop the drum without causing excessive stress.

The drum release system includes the drum release actuator and drum lock bracket assembly. Each actuator has two M-130 squibs, though either squib firing alone will cause a successful actuation. The squibs fire into a chamber, moving a piston which in turn pulls a pin to release the drum from the full out position. The lock bracketry on the coarse control drum, which engages the lockout pin, incorporates a safety feature which prevents removal of the ground safety lock if the pin is not engaged with the control drum. The safety feature is a spring-loaded clip which is inserted into the locking arm of the ground safety lock when the lockout pin is not properly engaged. The ground safety lock is described in Paragraph IV-D.

The unique features of the fine control drum package include its drum release system, the control drum actuator, position indicator, and gear linkage.

The drum release actuator in the drum release system is identical to the one in the coarse control drum package. Since the brake on the control drum actuator prevents insertion of the drum even though the lockout pin is removed, the spring-loaded safety feature mentioned above for the coarse control drum is not incorporated in the drum lock bracketry on this drum. The bracketry does include a forked slide which may be disengaged to allow 2° of drum movement with the lockout pin and ground safety lock in place. This permits a check of the control system on the launch pad. During the boost phase, this slide will be engaged to hold the drum immobile.

The control drum actuator is a motor that rotates in finite steps. The windings are each connected in series with a brake on the motor shaft. When a signal is received from the controller, the brake is released and the shaft turns a finite distance. Four motor steps complete one duty cycle and rotate the control drum 0.5° ± 0.1°. Each time the motor is operated, a full duty cycle is completed.

Two gears link the control drum actuator to the control drum. The pinion gear attached to the motor shaft is made of Haynes Stellite 6B, and the gear segment attached to the drum is made of titanium. These gears are matched sets which limit the backlash to 0.1° drum rotation at all times. A Molykote X-15 layer is used to prevent self-welding of the gears.

The position indicator in the fine control drum package is provided for diagnostic instrumentation only. The output voltage of the indicator varies with drum position to give the desired position information. Two ranges of operation are provided; a coarse range indicating position between 0 and 135° and a fine range indicating position between 0 and 30° from the full in position.

B. SUPPORT SYSTEM

The control and reflector assembly is mounted on the reactor in two halves. Each half is supported on two hinges located at the lower end of the assembly. The halves are rotated into position on the hinges until stops located near the top of the reactor are contacted. The complete assembly is then held in position by a band around the upper end of the reflector halves.

Both hinges on a side are of a similar design, although one is restrained against lateral motion while the other is free to allow thermal expansion. Each hinge sits on a 1/4-in.-diameter pin attached to the reactor structure. The hinge is held down by a 3/8-in.-diameter pin attached to the reactor structure that bears on a cylindrical surface concentric with the 1/4-in. diameter pin. The 3/8-in.-diameter pin is an eccentric pin and can be adjusted to obtain the proper clearance in the hinge. Ejection springs, described in Paragraph IV-C, push upward on the reflector so that the 3/8-in.-diameter pin and the cylindrical surface will always be in contact except during launch when maximum accelerations are present. Coatings are used on the hinge to prevent self-welding.

Positioning bolts are used on the upper end of the reflector assembly to adjust the position of the assembly. These bolts bear against the stop brackets attached to the reactor vessel. Again, coatings are used to prevent self-welding.

The band used to hold the assembly in place incorporates two springs to maintain the band tension within tolerance at all times. The tension of the band is set at 165^{+15}_{-10} lb at ambient conditions. During launch, the band will be heated to a temperature greater than the beryllium reflector, but the springs will maintain sufficient tension to overcome acceleration forces. During thermal acceptance

testing and operation, the band will be cooler than the beryllium reflector, but the springs allow stretching of the band without increasing tension in the band to the yield point. Thus, the band is reusable after the thermal cycles expected prior to launch.

The reflector assembly is mounted 0.026-in. off center from the reactor at ambient conditions with a nominal gap of 0.070-in. between it and the vessel. During startup, the beryllium temperature rises much slower than the reactor temperature. When the reactor first reaches full power the gap is reduced to a nominal 0.040 in. At this time the reflector will be concentric with the reactor as relative thermal expansion takes place from the hinges fixed against lateral motion. These hinges are located 3-1/2-in. off the reactor centerline. During steady-state operation the gap between the reactor and beryllium will have increased to 0.055 in. and the reflector will be 0.014 in. off center from the reactor.

C. EJECTION SYSTEM

Reactor shutdown may be effected by ejection of the control and reflector assembly. Ejection is accomplished by compression springs located at the bottom of the reflector halves. When the retainer band is released, the reflector halves are pivoted outward around their support hinges by the spring force.

Prior to ejection of the thermal shield, the reflector halves can be rotated outward at least 7° by releasing the retaining band. After the thermal shield is ejected, the reflector halves can be ejected completely away from the reactor. The two reflector halves will still be connected to the reactor by the electrical wiring. Seven degrees outward rotation of the reflector reduces reactivity by about $17.00, and complete reflector ejection reduces reactivity by $20.30.

Two ejection springs are used for each reflector half. These Rene 41 compression springs are located beneath the reflector adjacent to the reflector halves separation. Each spring exerts 100 ± 5 lb on the reflector at room temperature, and 85 ± 5 lb at operation temperature.

The hinges are described in Paragraph IV-B. When the reflector rotates outward about 15°, the 3/8-in.-diameter pin disengages from the cylindrical surface allowing the two parts of the hinge to completely disengage.

Three distinctly different signals are used to initiate reflector ejection. All three signals activate an electrical device which releases the reflector retainer band. An electrical signal can be provided: (1) by ground command through an umbilical prior to liftoff, (2) by telemetry, or (3) by a failure-sensing device (low converter output voltage). The failure-sensing device starts a 1-min timer which resets if the malfunction signal is removed. If the signal persists, a 1-hr delay timer is started. This in turn triggers the electrically actuated band release device. The electrically actuated band release device consists of one cylinder inside another brazed together with a low temperature melting alloy. These cylinders house a small electrical heater which receives power when the ejection signal is received. The band release device is built into the retainer band. When the heater raises the temperature of the braze to its melting point (approximately 1250°F), the two cylinders are pulled apart, severing the band. The 1/2-in. overlap of the two cylinders is less than the available stroke of the two springs in the band, thus the springs ensure complete separation of the device.

A mechanical device is also used to separate the reflector retaining band. This mechanical device is activated by a drop in temperature of the NaK in the outlet line adjacent to the reactor. The temperature actuated band release device works on the principle of differential thermal expansion of two materials. In this design a steel rod is used inside a molybdenum tube. While the temperature is increasing, the steel rod, which has a much higher coefficient of thermal expansion than the molybdenum, is allowed to grow freely relative to the tube. On decreasing temperature, the rod is gripped and placed in tension as it tries to decrease in length relative to the tube. With a temperature drop of 350 ± 100°F the tension becomes great enough to break a bolt holding the retainer band together. A temperature drop of greater than 500°F at the location of the device can occur in one of two ways: (1) if the NaK flow stops, or (2) if the system is penetrated and all NaK is lost.

The retainer band is also designed to release upon reentry heating if reflector ejection has not already occurred. The brazed joint in the electrically actuated band release device will melt at about 300,000 ft thereby releasing the reflectors. If for some reason this does not occur, the entire band will melt at about 285,000 ft resulting in reflector ejection.

D. GROUND SAFETY SYSTEM

A ground safety lock as shown in Figure 13 is provided for each control drum. These locks are operated with a key and will be removed during the "count-down" sequence. When installed and locked, an arm positively prevents insertion of the control drums. These locks will be in place during all shipping and ground handling operations. The locks on the coarse control drums cannot be removed unless the squib-actuated lockout pin is engaged.

Removal of the ground safety locks will be one of the final operations prior to launch. Access holes are provided in the nose cap to allow removal after all squibs have been installed and the nose cap is put in place.

Prior to installing the nose cap over the SNAP unit the control drums are restrained by void filler blocks. These devices are capable of maintaining the reactor subcritical when the reflectors are installed and the reactor is surrounded by infinite water. Figure 14 illustrates the void filler configuration.

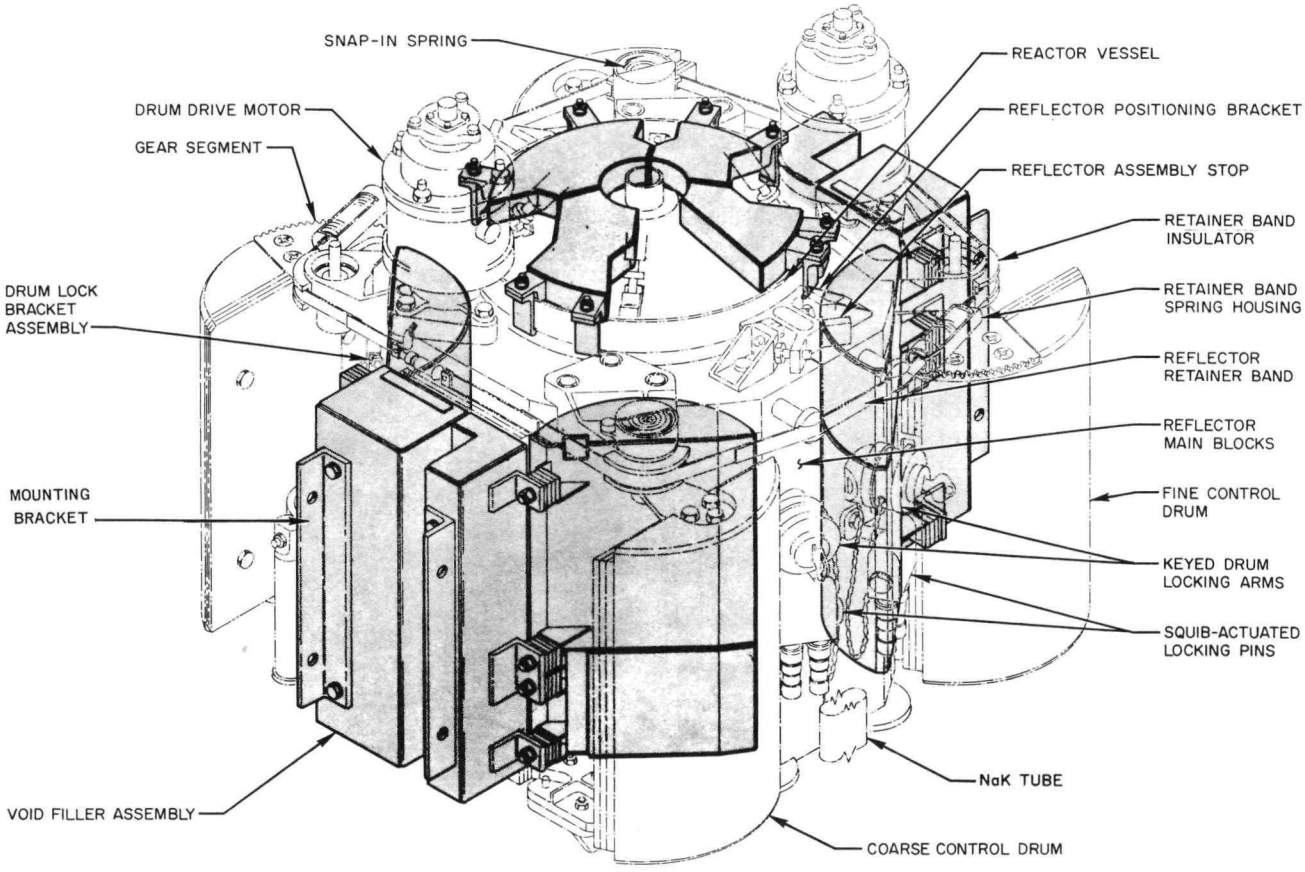

6-27-63 7561-0513A

Figure 14. SNAP 10A Void Filler Assemblies

BLANK

V. REACTOR CONTROL

A. INTRODUCTION

The functions of the control system are (1) to control the rate of reactivity insertion during the startup procedure, (2) to establish operation stability at design levels, and (3) to reduce reactivity to a subcritical condition at termination of the mission.

Because of the small size of the reactor, about 40% of the neutrons born in the fission process will leak away from the core unless it is surrounded by an adequate neutron reflector. Thus, complete control of the reactor is achieved simply and efficiently by varying the effective thickness of the neutron reflector surrounding the core. The reflector is a hollow cylinder of beryllium with a wall thickness of approximately 2 in. Four semicylindrical drums comprise a portion of this cylindrical wall of beryllium. Rotation of the control drums has the effect of varying the thickness of the reflector, thus permitting startup and control of the reactor.

B. SYSTEM OPERATION

After orbit has been established, startup command is given by T/M. This signal energizes the "on" coils of the startup relays. Switching these relay contacts energizes the controller relay "on" coils, thus switching their contacts and supplying unregulated 28 v dc and plus and minus regulated 28 v dc power to the controller. At the same instant, the control drum squibs are fired releasing the drums. Coarse control drum "in" limit switches provide telemetered verification.

The controller starts to drive the two fine control drums in at the rate of $1/2^{\circ}$ each 150 sec. The controller will continue to drive the control drums in until the reactor outlet thermal switches close (1010 ± 10 °F). These switches are located on the reactor NaK coolant outlet line. This event will occur approximately 9 hr after the start command. For the following 72 hr, during which the reactor reaches equilibrium, the controller is maintained in an active condition. It drives the drums in if the reactor temperature drops below the temperature switch setpoint. (The reactor outlet temperature switches open when the temperature drops below the setpoint.) Electrical power is then removed to deactivate the controller which can be reactivated by T/M command.

Diagnostic instrumentation is provided for status information. Variable position sensors are mounted on the two fine control drums. Limit switches provide "full in" and "full out" status on both the fine and coarse control drum. Limit switches also provide "on" and "off" status on each half of the reflector assembly and on the retaining band.

End of mission can be initiated by a malfunction signal from the converter system or by T/M command. The termination signal activates a 1-min timer. This timer will reset to zero if the termination signal is removed before the 1-min period is completed and thus will prevent termination due to short-time malfunction indications. If the termination signal is still present at the end of one minute, this timer activates a 1-hr timer. The purpose of the 1-hr timer is to allow acquisition of diagnostic data prior to reactor deactivation. At the end of the 1-hr period, electrical power is applied to the electrically actuated reflector band release device to break the reflector retaining band. This allows the reflector to be ejected, thereby reducing the reactor to a subcritical condition.

C. CONTROL COMPONENTS

Components comprising the reactor control system are:

1) Controller

2) Controller drum actuators

3) Thermal switches

4) Timer (1-hr and 1-min combined)

5) Electrically actuated band release device

These components are described as follows.

1. Controller

The reactor controller (see Figure 15) is a digital device which provides four sequenced power steps to the control drum actuators every 150 sec when the temperature switches indicate that the reactor outlet temperature is below the temperature setpoint. The controller employs transistorized logic throughout with the exception of the output power switches which are relays. The internal frequency source or time base is a transformer-coupled multivibrator.

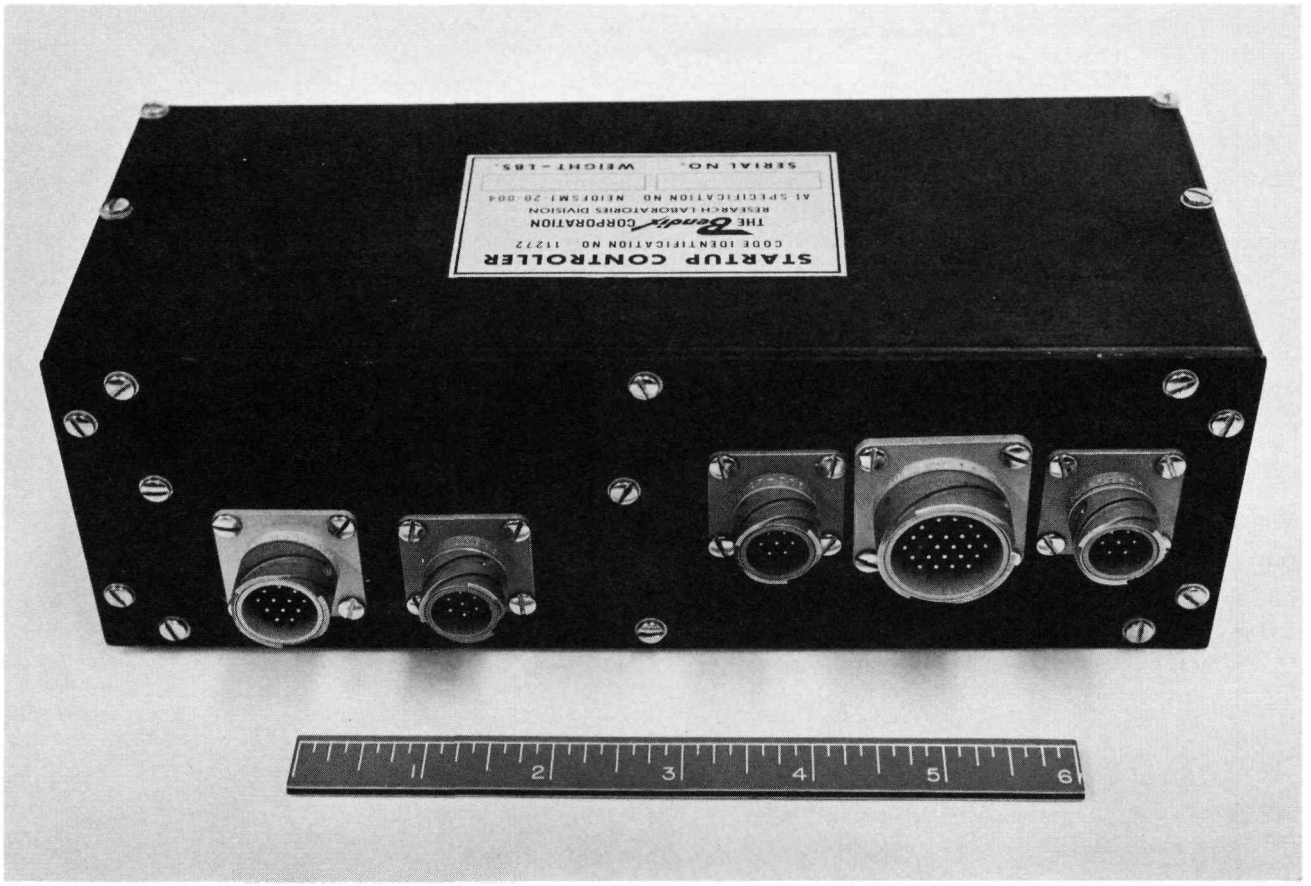

6-26-62 7580-5560D

Figure 15. Reactor Controller

The primary reason for the 150-sec time delay period between successive 1/2° drum rotations is to allow time for the reactor temperature to respond to the increase in reactivity. This stepping rate produces a reactor startup time compatible with the reactor characteristics, startup battery capacity, and temperature transient capabilities of the nuclear power system.

2. Control Drum Drive Actuators

The control drum drive actuator is required to rotate the drum in small (1/2°) increments. A stepper motor is used, together with a single 13.8:1 gear set. The motor is a synchronous machine, with a permanent magnet rotor and a 2-phase stator. The rotor and stator are notched to form 50 and 48 teeth on each respectively. The mismatch produces the effect of 200 poles. Therefore, with each change in polarity in the stator windings, the rotor will rotate 1.7°. Each phase of the stator is divided into two windings, which are wound in opposite polarity. This is done to allow simple ON-OFF switching to produce the effect of phase polarity reversal. At any time during actuation two stator windings are always energized. The direction of rotation is determined by the sequence in which the windings are energized. The actuator is designed to perform four steps in order to rotate the drum 1/2°. A 4-step sequence is used to allow the electronic circuits in the controller to return to a stable condition.

A solenoid-actuated brake is mounted in the upper end bell of the actuator, with the solenoid armature spring-loaded against a disc on the rotor shaft. The solenoid winding is in series with the stator, being connected to the common return of the four stator windings. Therefore, the brake is released when power is applied to the actuator and is reapplied when the actuator is deenergized.

3. Thermal Switches

Thermal switching required for control of the SNAP 10A is accomplished by a platinum resistance sensor coupled to an electronic switch. The resistance sensor is placed in a thermal well in the NaK outlet line above the reactor vessel head, and the switching unit is located in the SNAP unit instrument compartment.

Two switches in parallel are used for increased reliability.

4. Timer

The 1-min and 1-hr timer functions are combined in one unit. This is an electromechanical device. Figure 16 illustrates the external configuration.

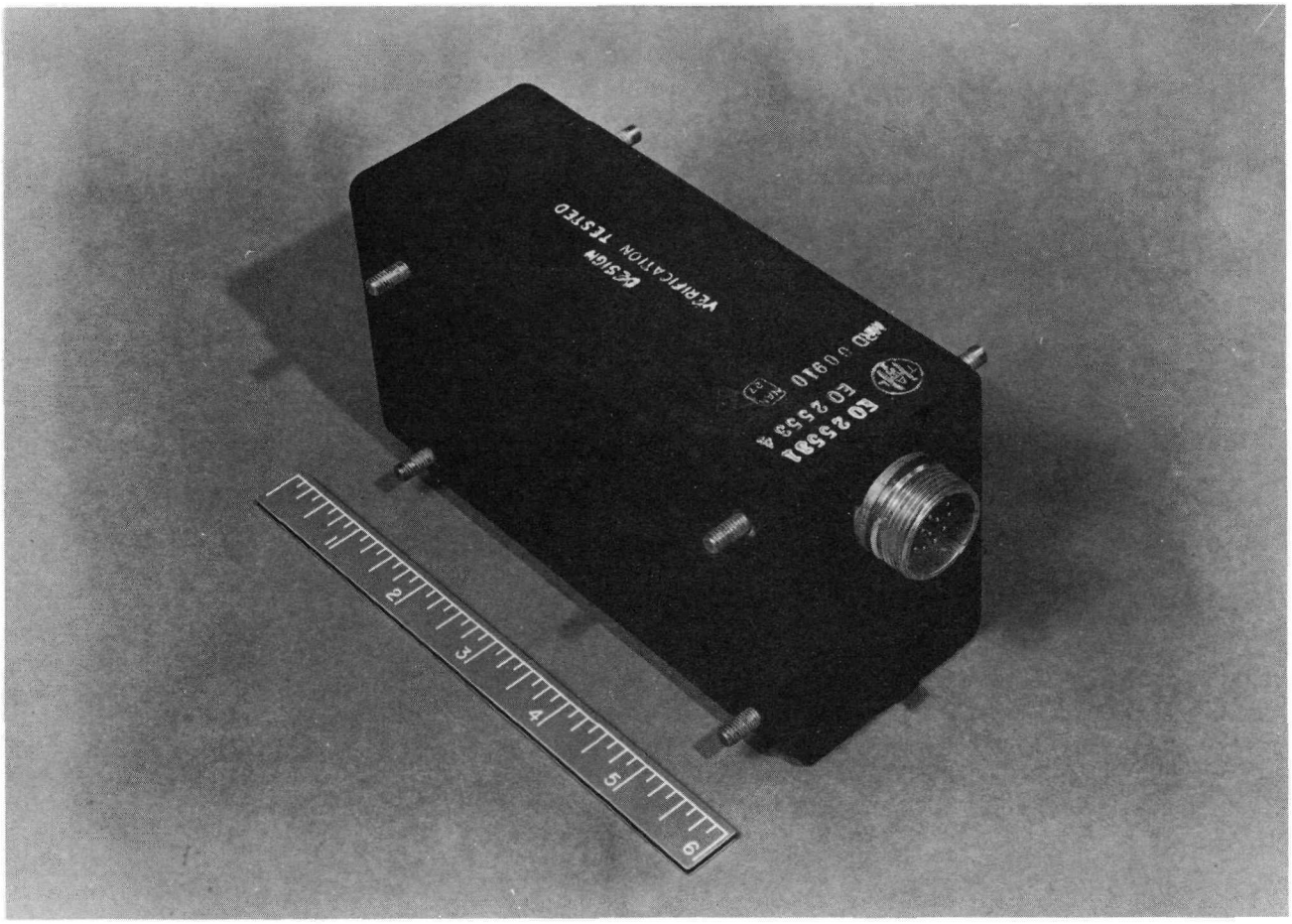

7-1-63 7623-5501

Figure 16. Delay Timer

5. Electrically Actuated Band Release Device

The electrically actuated band release device consists of a pair of concentric cylinders brazed with a material having a melting temperature of approximately 1250°F. Each of the cylinders is attached to the band so that the device is a link in the band. A resistance heater inside the inner cylinder heats the device to the melting point of the solder thereby allowing the cylinders to be disengaged by the band tension and reflector ejection spring loads.

D. POSITION INDICATING DEVICES

The following devices provide position status of various components of the reflector assembly for diagnostic information:

1) Control drum position sensor and demodulator

2) Position switches

These are described as follows.

1. Control Drum Position Sensor and Demodulator

The control drum position indicators are rotary differential transformer devices directly coupled to the drum shafts by zero backlash couplings. Power input to these units is 26 v 400 cycle supplied by a stepdown transformer located in the instrument compartment. The output signals from the position sensors are the inputs to two demodulators. Each demodulator has two 0- to 5-v dc outputs. A coarse scale indicates drum position from 135 to 0° and a fine scale indicates drum position from 30 to 0°.

2. Position Switches

Twelve position switches are used on the reflector assembly. These are:

Coarse Control Drum No. 1 in limit (PnS-1) and out limit (PnS-2)

Coarse Control Drum No. 2 in limit (PnS-3) and out limit (PnS-4)

Fine Control Drum No. 1 in limit (PnS-5) and out limit (PnS-6)

Fine Control Drum No. 2 in limit (PnS-7) and out limit (PnS-8)

+Z reflector assembly position on-off (PnS-15)

-Z reflector assembly position on-off (PnS-16)

+Z reflector band on-off (PnS-17)

-Z reflector band on-off (PnS-18)

These switches are of the high temperature nonsealed single-pole double-throw type. When a second pole is required, two switches are used.

VI. FUEL

The reactor fuel material is a hydrided zirconium-uranium alloy. The alloy contains 10 wt % uranium and is hydrided to a nominal N_H of 6.35×10^{22} atoms of hydrogen/cm^3 of fuel. This material is formed into rods of 1.21-in. diameter and 12.25-in. length and is canned in Hastelloy-N cladding tubes. The cladding tubes are 1.25-in. OD and have a wall thickness of 0.015 in. Internal surfaces of the cladding tubes are coated with a 2.5 to 3.5 mil layer of ceramic glass material. This coating acts as a barrier to hydrogen leakage from the fuel. The ends of the fuel elements are sealed with end caps of Hastelloy-N material welded to the cladding tube. The end pins which position and hold the elements between the grid plates are an integral part of the end caps. Each fuel element weighs 3.4 lb and has an overall length, including end pins, of 12.82 in. The fuel/moderator element is shown in Figure 17.

Each unclad fuel rod contains approximately 128 grams of U^{235}, 11.8 grams of U^{238}, 24.6 grams of hydrogen, and 1215 grams of zirconium. Total weight is approximately 1380 grams (3.04 lb). A small amount of carbon (approximately 0.15 wt %) is added as a grain refiner to produce a stronger rod. The fuel is a hard semibrittle material with a metallic appearing machined surface. All edges of the fuel rod are rounded to prevent damage to the ceramic hydrogen barrier during assembly and handling of the fuel element.

The ceramic glass hydrogen barrier prevents excessive loss of hydrogen from the fuel rod operating in the high temperature and high radiation environment of the reactor core. Integrity of this barrier must be maintained. Hence, handling and shipping of fuel elements must be accomplished with suitable precautions to prevent damage due to excessive shock or vibration.

The ceramic glass barrier is composed primarily of oxides of aluminum, silicon, titanium, manganese, and barium with smaller amounts of sodium, lithium, and potassium. This ceramic coating is generally applied in three firings. In the last two firings a small quantity of samarium oxide (Sm_2O_3) is incorporated into the coating. The samarium is a burnable poison. Depletion of this material inserts sufficient reactivity at the proper rate to provide more than 1 yr of stable reactor operation.

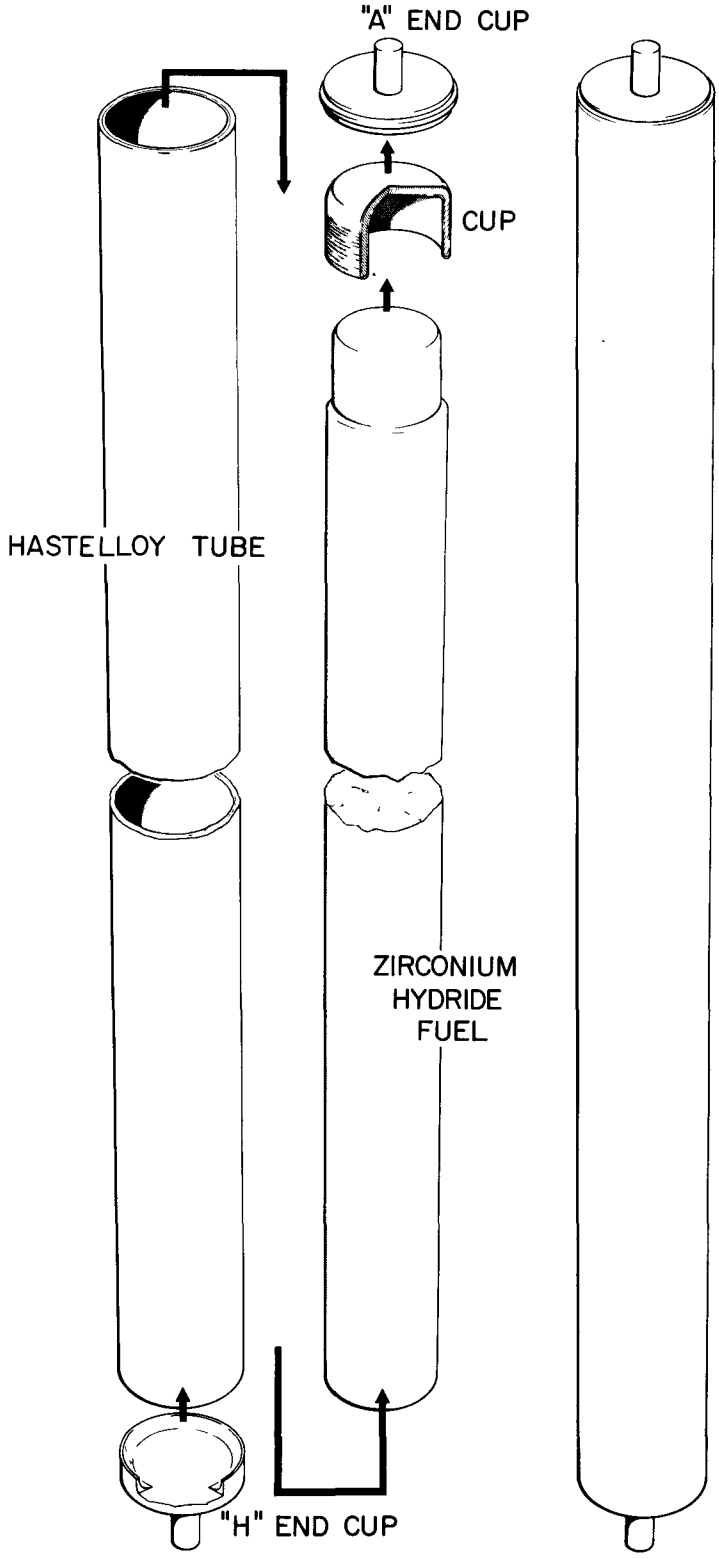

9-28-61 7550-20211

Figure 17. SNAP 10A/2 Fuel Element

One end cap of the fuel element is welded to a cladding tube prior to application of the ceramic barrier. After the ceramic barrier is fired, a fuel rod is inserted into the cladding tube. The cladding tube is then sealed against hydrogen loss by insertion of a ceramic coated blend cap. The hydrogen barrier is made complete by locally heating the cladding tube and blend cap to blend the ceramic surfaces together. Following the blending operation, an end cap is welded to the cladding tube, covering the blend cap. No end play exists between the fuel rod and cladding tube.

A small number (less than 10) of the 37 fuel elements required for a SNAP 10A core loading will have a nominal hydrogen content of 6.0×10^{22} atoms/cm^3 of fuel. These special low hydrogen content elements are used to adjust the excess reactivity of the core. Low N_H elements are identical to the standard element except in hydrogen content.

BLANK

VII. OPERATING CHARACTERISTICS

The SNAP 10A reactor is similar in nuclear design to the test and developmental reactors which have been developed, or are presently being operated by, Atomics International for the Atomic Energy Commission.[1, 2, 3] The SNAP Experimental Reactor (SER) has been extensively tested and its nuclear characteristics determined. After 6000 hr of operation, the SER was disassembled and the SNAP Developmental Reactor (SDR)[3] placed in operation. The SDR logged over 11,000 hr prior to being shut down. These two operating reactors, along with the SCA-4B and SCA-4C critical experiments, have provided a wealth of experimental information regarding nuclear characteristics. Nuclear characteristics of the SNAP 10A reactor have been determined analytically mainly through use of the AIM-6 multigroup diffusion code with the Los Alamos 16-group cross section library. The AIM-6 code is an expanded version of the WANDA code, incorporating a greater group structure and other features and operations which have been found desirable.[4] The basic AIM-6 calculations have been found by experience to agree reasonably well with SNAP experimental data. Additional nuclear calculations have been made using the ZOOM, CURE, ULCER, and SNG codes.[5,6,7,8] Fast neutron and gamma shielding calculations have been made using the FARSE 2, SCAR 1, and 14-0 codes.[9,10,11] A summary of SNAP 10A reactor design, nuclear, kinetic, shielding, and weight characteristics is presented in Table I. Most of the nuclear parameter information summarized in Table I (Section I. E.) is based on experimental data obtained from SER, S2DR, or the SCA critical experiment. The remaining parameters have been calculated using the AIM-6 or other nuclear codes. Only calculated radiation dose information is presented in Table I; experimental verification of shielding calculational methods is now in progress.

Figure 18 shows the anticipated long-term temperature drift of the SNAP 10A reactor. During the first three days of operation, the reactor outlet temperature will be controlled through inward rotation of the beryllium control drums. The reactivity changes due to temperature and power defect, xenon buildup, and partial hydrogen redistribution take place during this period. At the end of 72 hr, control drum movement ceases and the reactor operates on passive control for the remainder of the 1-yr operating period. For the first month of passive control period, system reactivity (and therefore temperature) drops as

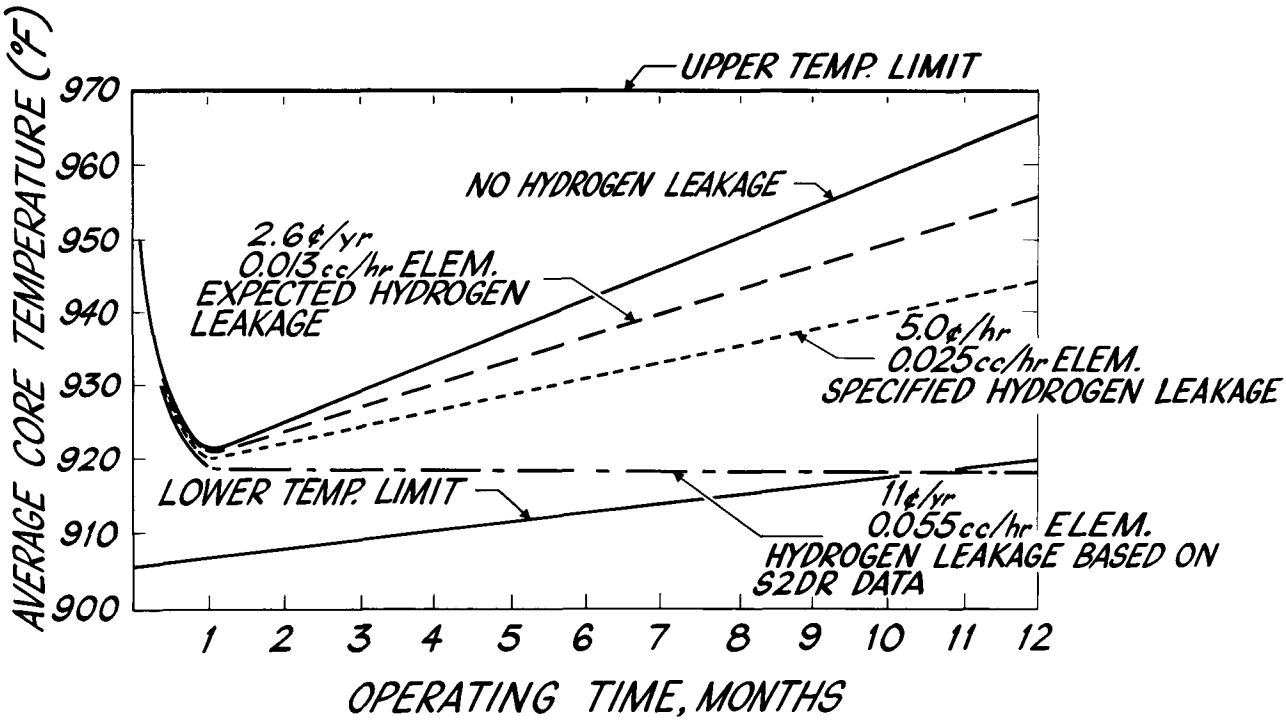

8-27-63 7561-0296A

Figure 18. Long-Term Temperature Drift of SNAP 10A Reactor

the negative reactivity effect accompanying hydrogen redistribution rapidly reaches its maximum value. Following completion of hydrogen redistribution, core temperature slowly rises as the positive reactivity insertion caused by samarium prepoison burnout more than balances the reactivity losses due to fuel depletion, fission product accumulation, and hydrogen loss.

Reactivity values of the SNAP 10A reactor in various normal and abnormal configurations and environments form an extremely important part of the safety analysis. In addition, they govern to a large measure the formulation of safe handling procedures and emergency plans.

SCA-4C paraffin block experiments have shown that the worth of one human leaning against the reactor surface is approximately 30¢ for reflected cores and about $1.10 for a bare reactor. However, the rigid rectangular blocks do not represent the more flexible contours and appendages of the human body which occur during reactor assembly operations. Additional experiments involving use of a hydrocarbon plastic human mockup, which could be draped over and around the reflected reactor, were performed to obtain effects of a simulated flexible human body.

The mockup was prepared by packing 200 lb of plastic pellets and paraffin into a pair of coveralls. Two long rubber gloves, representing arms, were also filled with the plastic pellets. It was found experimentally that the mockup was worth about $0.85 when leaning against and over the reflected reactor. The total worth increased to approximately $1.95 when "arms" were inserted as far as possible into open drum voids.

The reactivity information summarized in Tables IV and V is therefore based on three separate cases of potential human body reflection:

a) Single human body - standing adjacent

This configuration corresponds to a single person standing against the reactor core or reflector, as the case may be, without any placement of hands in the drum voids. These reactivity values are based on the paraffin block experiments.

b) Single human body reflection - wrap around

This estimate is based on what is believed to be the maximum possible worth of a human body, even with intentional motives. It is therefore considered to be an absolute upper limit for one person. For reflected reactor configurations, results of the human mockup experiments have been used. With bare reactor cores, human body worths, which are 1/3 those of infinite radial water reflection have been chosen to represent an upper reactivity limit.

c) Maximum human body reflection

This case is an extension of b) above, without limit to the number of persons involved (at least three). The reactivity worth associated with maximum human body reflection represents an absolute upper limit to the reactivity that can be added to the SNAP 10A system by any number of people.

The range of reactivity values provided in Tables IV and V for those cases where human body reflection is involved is based on the various human-reactor configurations discussed above.

A set of reference values both analytical and experimental is given in Tables IV through VIII.

TABLE IV

SNAP 10A REACTIVITY VALUES ($) UNDER VARIOUS ABNORMAL CONDITIONS DURING ASSEMBLY AND SHIPMENT

Condition of Reactor		Reactivity					
On Right Side	On Left Side	In Air	Single Human Standing Adj.	Single Human Wrap Around	Maximum Human Wrap Around	Infinite Water Reflection	
						NaK in Core	H_2O in Core
sleeve	sleeve	-19.40	-19.10	-17.40	-13.40	-10.20 ± 1.20	-3.00 ± 0.50
sleeve	bare	-20.50	-20.20 -19.40*	-18.50 -13.50	- 7.00	- 3.60 ± 2.00	4.20 ± 2.00
sleeve	reflector with void-filler blks	-12.70	-12.40	-10.70	- 8.20	- 6.00 ± 2.00	1.30 ± 2.50
reflector with void-filler blks	reflector with void-filler blks	- 6.00 ± 1.00	- 5.70	- 5.00	- 3.00	- 1.50 ± 0.50	5.60 ± 1.50
reflector with void-filler blks	bare	-13.80	-13.50 -12.70*	-12.80 - 6.20*	- 1.80	0.60 ± 1.50	7.90 ± 2.00
bare	bare	-21.70	-20.60	-14.70	- 0.70	3.00 ± 0.80	10.30 ± 1.50

*Human on bare side

TABLE V

REACTIVITY VALUES ($) FOR BERYLLIUM-REFLECTED SNAP 10A – NO VOID FILLER BLOCKS

Beryllium Reflected Reactor – All Drums Out No Void Filler Blocks	-6.13
Single human body reflection – standing adjacent	-5.78
Single human body reflection – wrap around	-4.20 ± 1.00
Two human body reflection – wrap around	-2.25 ± 1.00
Maximum human body reflection	0 ± 1.50
Water in core – no water reflection	1.20 ± 0.79
Infinite water reflection – no water in core	7.10 ± 2.00
Infinite water reflection and water in core	14.40 ± 3.00
Agena nose shroud and cap in place (launch config.)	-6.08
Beryllium Reflected Reactor – Two Drums In No Void Filler Blocks	-1.73
Single human body reflection – standing adjacent	-1.38
Single human body reflection – wrap around	+0.20 ± 0.50
Maximum human body reflection	+3.70 ± 1.50
Infinite water reflection – no water in core	8.30 ± 2.00
Infinite water reflection and water in core	15.60 ± 2.00
Infinite half plane water reflection (no core water)	0.70 ± 2.00
Agena nose shroud and cap in place (launch config.)	-1.68

TABLE VI

REACTIVITY VALUES ($) FOR BARE SNAP 10A REACTOR UNDER SEVERAL ABNORMAL CONDITIONS
(See Table IV for additional bare reactor data)

Bare Reactor – NaK in Core	
Infinite half plane water reflection	-8.00 ± 2.00
Infinite half plane sand reflection 0% H_2O	-18.00 ± 2.00
Infinite half plane sand reflection 30% H_2O	-12.00 ± 2.00
Infinite half plane concrete reflection	-12.00 ± 2.00
Bare Reactor Completely Submerged in Sand – Moisture Content for Criticality – NaK in Core	35% ± 5%
Bare Reactor – Water in Core, No Water Reflector	-14.40 ± 1.00

TABLE VII

NORMAL SNAP 10A REACTIVITY WORTHS, TEMPERATURE, AND POWER COEFFICIENTS

Normal Reactivity Worths

Material	Worth	Remarks
Hydrogen	64¢ per wt % Hydrogen	Small Changes in Fuel Loading
U^{235}	9.1¢ per wt % U^{235}	Small Changes in Fuel Loading
Zirconium	15.6¢ per wt % Zr	Small Changes in Fuel Loading
NaK (in core)	$0.09 ± 0.10	Estimated
Central Fuel Element	$3.15 ± 0.05	SCA-4A Data with Be Reflector
Edge Fuel Element	$1.55 ± 0.05	SCA-4A Data with Be Reflector
Shield	$0.35 (extrapolation)	

Temperature and Power Coefficients

	Value	Remarks
Fuel Temperature Coef.	-0.07 to -0.13¢/°F	-0.10¢/°F Probable Value
Total Temperature Coef.	-0.22¢/°F	Average Value
Power Coefficient	-0.4¢/kw	Average Value

TABLE VIII

OPERATIONAL SNAP 10A REACTIVITY DATA

Condition	Reactivity ($)	Remarks
Reactivity Data for ATF (Bldg 019)		
Be Reflected Reactor (Dry) Including Vault Effect		
Four Drums In	+2.80	75°F Average Temperature
Three Drums In	+0.60	75°F Average Temperature
Two Drums In	-1.60	75°F Average Temperature
One Drum In	-3.80	75°F Average Temperature
All Drums Out (No Void Fillers)	-6.00	75°F Average Temperature
All Drums Out (Void Fillers	-5.50	75°F Average Temperature
Required Excess Reactivity at 75°F with NaK	+2.70	All Drums In
Required Zero Power Excess Reactivity at 968°F Includes	+0.72	All Drums In
Bldg 019 Vault Worth	+0.03	
Power Defect	-0.13	
Bldg 024 Vault Worth	+0.02	
Recommended Excess Reactivity in Space at 950°F, Full Power, 72 Hr after Startup	+0.40	

VIII. REACTOR CORE

A. DESIGN

The SNAP 10 reactor core is composed of 37 moderator-fuel elements. These elements are arranged in a triangular array, on 1.26-in. centers, to form a core which is hexagonal in cross section. The overall dimensions of the core are: 9 in. across the corners, about 8 in. across the flats, and 12-1/4 in. in length.

The core assembly is contained in a cylindrical reactor vessel of Type 316 stainless steel. The vessel is 9 in. in diameter, 16 in. in length, and has a minimum wall thickness of 0.032 in. Internal side reflectors of beryllium are used to round out the hexagonal core configuration and fill the void spaces in the core vessel.

The elements are positioned in the vessel between grid plates of Hastelloy-C material. End pins, 0.242 and 0.180 in. in diameter, engage holes in the upper and lower grid plates respectively to position the elements in the core. The lower grid plate is supported by a ring at the bottom of the reactor vessel. The top grid plate is spring-loaded against the vessel top head to permit thermal expansion of the core in the axial direction.

All coolant flow through the core is through the interstices formed by adjacent fuel elements or by elements and the internal side reflectors. Coolant passes through the grid plates by means of 3/8-in. diameter coolant holes drilled to align with the core coolant passages.

An orifice plate located below the lower grid plate was designed to produce the desired flow distribution. The desired flow distribution is one which produces equal coolant temperature rise in all coolant channels and a constant outlet temperature profile across the core. The coolant plenum chambers located above and below the core assembly in the vessel provide mixing space for the coolant.

B. THERMAL AND HYDRAULICS ANALYSIS

1. Core Flow Distribution

Coolant enters the reactor via two diametrically opposed inlet nozzles below the lower grid plate. The velocity of entry is 3.2 ft/sec in a direction

normal to the axis of the reactor. After entering the reactor vessel, the flow decelerates and turns to enter the core. The lower grid plate is made up of two plates: a support plate and an orifice plate. The coolant first flows through the orifice plate which contains 72 holes of diameters ranging from 1/4 to 3/16 in. in steps of 1/64 in., giving five different orifice sizes. The orifice plate was designed to provide a flow distribution to match the radial core power distribution. After passing through the orifice plate, the coolant enters the core through seventy-two 3/8-in. holes in the support plate.

The composite plate provides a rigid but lightweight support for the fuel elements and provides spacing between the orifice plate and the entrances to the coolant channels. If a single plate were used to support and orifice the core, the larger orifices would be partially covered and blocked by the fuel elements.

The core flow area is composed of the 72 orificed coolant channels and 12 extreme peripheral channels to which there is no entry from the lower plenum. The peripheral channels receive flow by crossflow between the fuel elements. NaK leaves the core through seventy-two 3/8-in. diameter holes in the upper grid plate. The flow converges upon the outlet nozzle in the center of the top head, and leaves the reactor at a velocity of 8.2 ft/sec.

Velocities in the coolant channels are governed by (1) the grid plate orifices, (2) the pressure drop in the channels, and (3) the amount of crossflow permitted by the nominal 0.010-in. clearance between fuel elements. Hydraulic tests of core velocity profiles were conducted using salt injection to measure average velocities. Shaping of the core flow was generally achieved, but the amount of crossflow could not be measured by this method. Analysis has shown that crossflow has a significant effect in reshaping the core velocity distribution downstream of the orifices. It is expected that by the time the coolant has traversed half the length of the core, the flow distribution will be nearly uniform. The importance of the core flow distribution upon fuel element temperatures can be assessed by a comparison of two limiting cases. First, in an ideally orificed SNAP 10A core, where the coolant flow profile exactly matches the radial power profile, the maximum fuel temperature in the core would be 1035°F. Second, if no orificing were provided and the velocity distribution were uniform, the maximum fuel temperature in the center fuel element would be 1080°F. These temperatures are based on an inlet temperature of 900°F. These temperatures show what little can be gained by perfect orificing of the SNAP 10A reactor and,

conversely, the effect that a 30% flow deficiency would have on fuel element temperatures. Since the higher of the temperatures is well below current temperature limits, and since the ideal flow distribution may not be achieved, much of the SNAP 10A analysis was based on the higher temperatures attained in a fuel element surrounded by flow-deficient channels.

2. Core Power Distribution

Because of symmetry of the SNAP 10A core and reflector, radial and axial power distributions are expected to be symmetrical about the core center. Local power peaking around the fuel elements is expected to be negligible. There is no significant reflector peaking in either the axial or radial planes. Because of small fractional burnup of fuel and resultant small control system movements, little change of core power profiles is expected during the design life of the reactor. For analysis purposes, axial and radial power distributions can be represented by the following expressions.

a) Axial Power Distribution — Normalized to an average axial power generation rate of 1.0.

$$P(z) = 1.47 \cos (1.48 - 0.241z), \qquad 0<z<12.25 \text{ in.}$$

b) Radial Power Distribution — Normalized to a peak radial power generation rate of 1.0.

$$P(r) = \cos 0.244r, \qquad 0<r<4.03 \text{ in.}$$

3. Fuel Element Temperature Distribution

a. Steady-State Temperatures

The highest fuel element temperatures and temperature gradients are attained in the center fuel element in the core. This element will be in the region of peak radial flux, and will exhibit the highest fuel temperature in the core. It will also produce the highest temperature rise in the adjacent NaK coolant. The latter would not be true for a perfectly orificed core; i.e., the coolant temperature rise would be the same in all channels. However, it is assumed that the flow rate adjacent to the center fuel element lies between the extremes produced by an ideally orificed core and an unorificed core. Temperature profiles in the fuel, clad, and coolant for the two extremes are shown in Figure 19 for a core inlet temperature of 900°F. The coolant profile has the "S" shape typically produced by a cosine axial power distribution. Clad surface temperature

exceeds coolant temperature due to a film drop of 2 to 26°F. Fuel surface temperature exceeds the clad temperature by an average of 15°F due to the temperature drop across the hydrogen-filled gap between fuel and clad. The average fuel temperature, averaged over the length and diameter of the fuel rod, is 1014°F for the higher temperature curves of Figure 18. The axial average clad temperature for the same curves is 987°F. These temperatures are used to evaluate the increase in the axial fuel-cladding clearance in Section VIII, B, 4b. At the point of peak fuel temperature, the average temperature across the diameter of the fuel is 1068°F; the adjacent clad temperature is 1037°F. These temperatures were used to evaluate the change in the radial clearance in Section VIII, B, 4b.

b. Temperatures During Startup

From ground to steady-state operating temperatures in orbit, the coefficient of expansion of the fuel clad material exceeds that of the fuel. Although the fuel-clad clearances increase from ground to operating temperature in orbit, the periods of maximum fuel-to-clad temperature during the startup transient require evaluation. The power, flow, and inlet temperature for the initial startup transient are shown in Figure 20. These curves span a 170-sec period during which the power peaks at 56 kw. Fuel-to-clad temperature excess in the center fuel element reaches a maximum 60 sec after the power peaks. At this time, and at a point 7 in. from the lower end of the fuel rod, the difference between the average fuel and the adjacent clad temperature reaches a maximum of 116°F (486-370°F). (See Figure 21.) At this time, the difference between the axial average fuel and clad temperatures on the centerline fuel element is 53°F (386-323°F) as compared to the steady-state difference of 29°F.

The minimum axial clearance occurs on an edge-of-core fuel element, 15 sec after peak power. Average fuel and clad temperatures for the core edge fuel element are shown in Figure 22.

To evaluate thermal stresses in the fuel rod, transient radial temperature distributions have been determined for the first 170 sec of the startup transient. Highest thermal gradients occur 7 in. from the lower end of the center fuel rod. Radial temperature distributions in the center element at this elevation are plotted in Figure 23. The temperature gradient increases to a maximum 60 sec after peak power (150 sec after initiation of transient) and

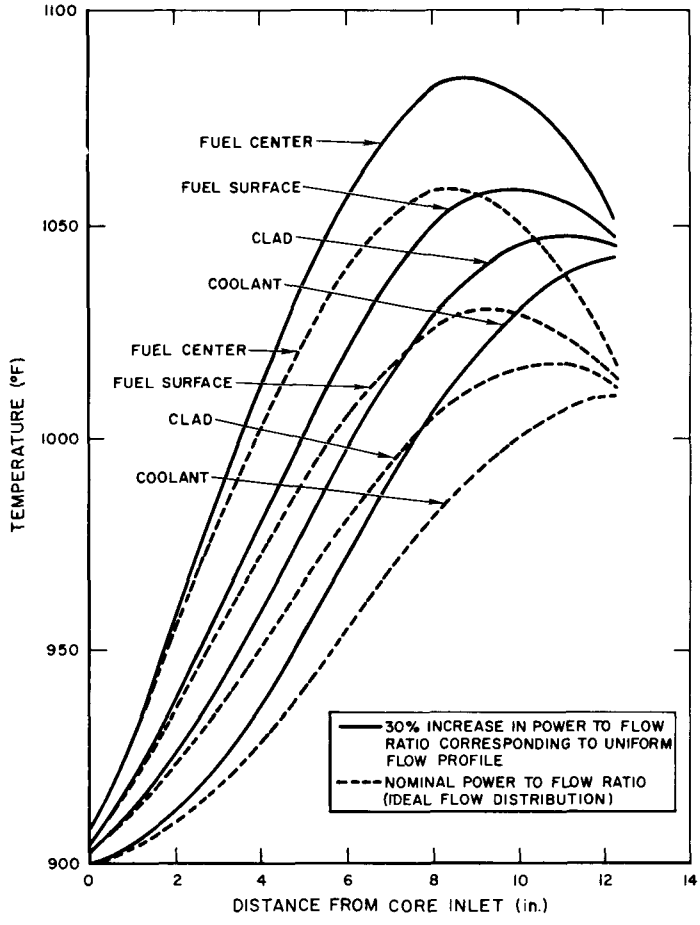

10-3-63 7623-0008

Figure 19. Steady-State Axial Temperature Distribution for Center Fuel Element-Comparison Between Ideal Flow Profile and Uniform Radial Flow Distribution (P = 34.7 kw, Flow 82 lb/min)

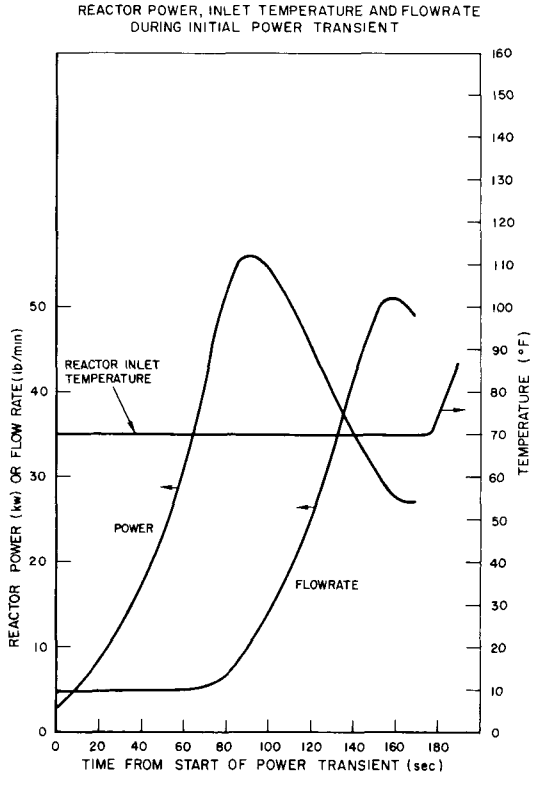

10-3-63 7573-1047A

Figure 20. Reactor Power, Inlet Temperature and Flowrate During Initial Power Transient

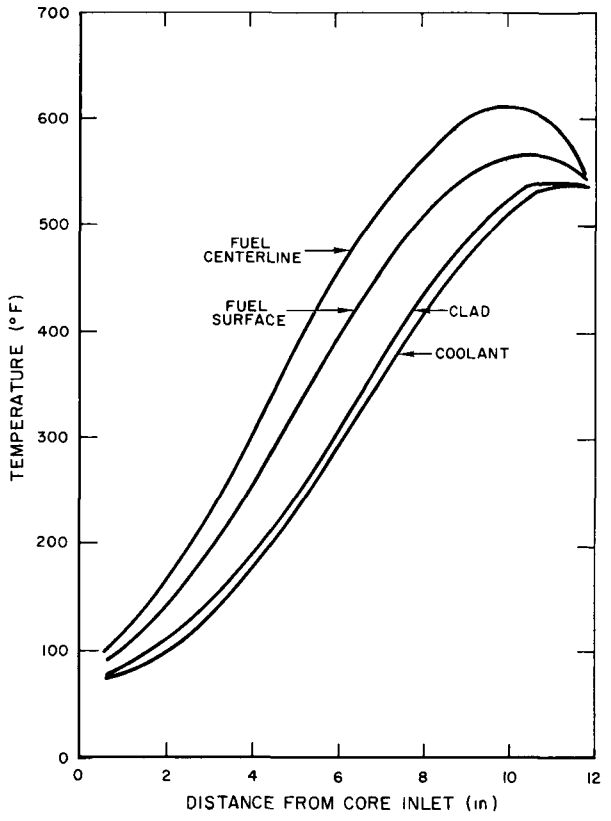

7-10-63 7623-0011

Figure 21. Axial Temperature Profiles in Center Fuel Element 60 sec After Peak Transient Power

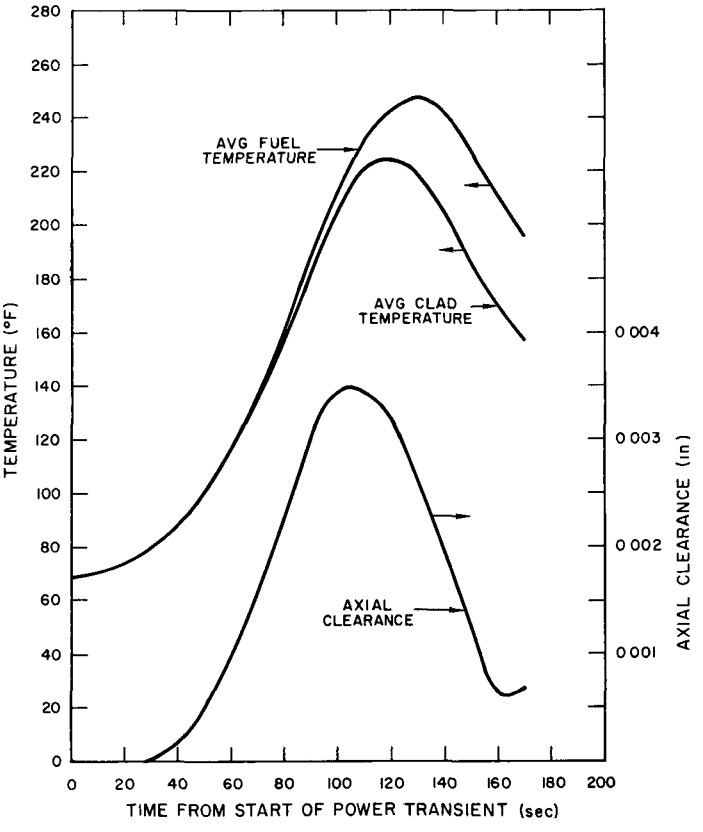

10-4-63 7623-0058

Figure 22. Average Temperatures and Axial Clearances for Core Edge Fuel Element During Initial Power Transient

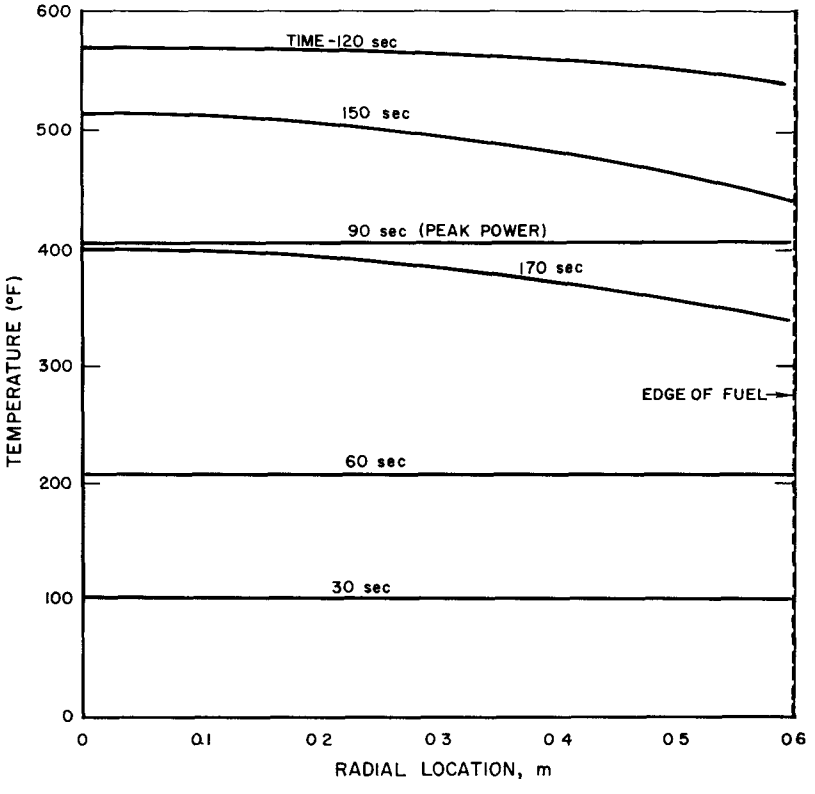

10-3-63 7623-0010

Figure 23. Radial Temperature Profiles in Center Fuel Element at 7 in. Elevation During Initial Power Transient (Time is relative to initiation of transient)

thereafter decreases. Peak stress occurs at the fuel surface where the temperature is lowest. Tangential stress at this point is +1550 psi; this value is well below the ultimate tensile strength of the fuel (σ_t > 15,000 psi at the local temperature).

Throughout startup and during steady-state operation, temperatures of the hydrogen barrier and the Hastelloy N clad differ by no more than 12°F. This can be shown by using a peak heat flux of 29,800 Btu/hr-ft^2 corresponding to the 56 kw peak power level during startup. For this heat flux, the temperature difference between the inside surface of the 0.0035-in. (maximum) thickness of barrier coating and the outer surface of the 0.0155-in. (maximum clad thickness is:

$$\Delta T = \frac{Q}{A}\sum\frac{\Delta X}{k}$$

$$= 29{,}800\left(\frac{.0155}{10.9(12)} + \frac{.0035}{1(12)}\right) = 12°F$$

The difference between the mean barrier and the mean clad temperature does not exceed 6°F.

A relatively severe temperature gradient exists during startup at the junction of the Hastelloy-N clad and the upper end cap. The difference between the average end cap and the clad temperatures, 0.1 in. below the end cap, reaches a maximum of 49.5°F in the centerline fuel rod 20 sec after the transient power peak. (See Figure 24.)

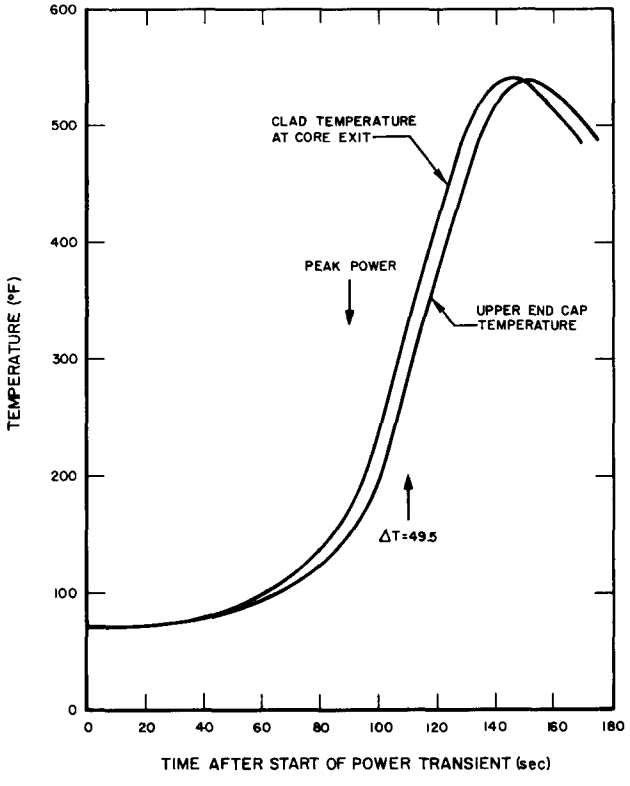

9-30-63 7623-0059

Figure 24. Centerline Fuel Element Upper End Cap and Clad Temperatures During Initial Power Transient

4. Differential Fuel-Clad Expansion

Thermal expansion data for the fuel and clad are illustrated in Figure 25. Note that the clad material expands somewhat more rapidly than does the fuel; the Hastelloy-N exhibits 29% more thermal growth between 70 and 1000°F.

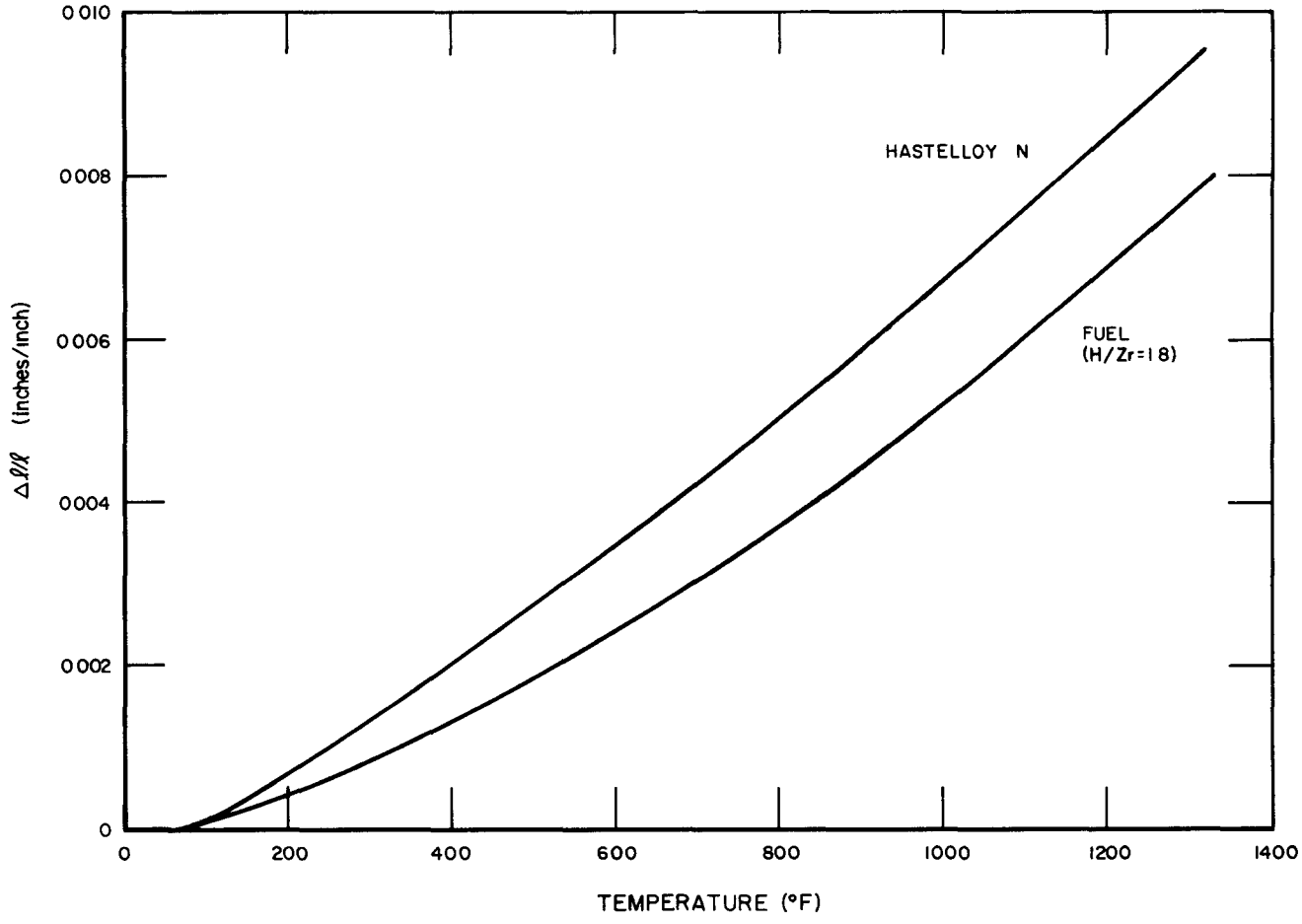

7-10-63 7623-0003

Figure 25. Thermal Expansion of S10A Fuel and Clad Materials

As a basis for evaluating the minimum clearances during operation, the minimum clearance at assembly were chosen. Combination of the fuel diameter and the coated tube ID (with their tolerances) yields a minimum diametric assembly clearance of 0.0035 in. The minimum axial clearance before welding of the end cap is zero.

a. Fuel-Clad Clearances During the Startup Transient

It was noted in Section VIII, B, 3b that the maximum fuel-to-clad temperature difference occurred during startup when the average fuel temperature in the center fuel element was 486°F and the clad temperature was 370°F. This was the worst local condition in the core, occurring 7 in. from the lower end of the fuel rod, 60 sec after the peak power transient. These temperatures produce a net increase in the diametric fuel-clad clearance of 0.00006 in. Using

the axial average temperatures for the edge fuel element discussed in Section VIII, B, 3b, the minimum axial fuel-clad clearance in the core during the startup power transient is 0.0006 in.

b. Fuel-Clad Clearances During Steady-State Orbital Operation

At the point of maximum fuel temperature in the center fuel element, the minimum steady-state diametric clearance between the fuel surface and the clad ID is 0.0015 in. greater than the clearance at assembly. Between room temperature and full power operation of the core, the axial clearance (as determined by the fuel and clad temperatures averaged along the length of the center fuel rod) increases by 0.0159 in. As long as a steady power level and flow rate are maintained, the average and local temperatures of the fuel must exceed the average and local clad temperatures. Therefore, there will always be a positive clearance between the fuel and cladding.

5. Differential Clad-Hydrogen Barrier Expansion

In Section VIII, B, 3b it was stated that the temperature excess of the hydrogen barrier over the clad temperature would not exceed 12°F during the life of SNAP 10A. Thus the assumption of essentially equal clad and barrier temperatures can be applied in determining the differential expansion at any point in the fuel element.

The combination of softening temperature of the barrier and operating temperatures in the fuel element produces compression in the barrier during fabrication and relaxation of barrier stress between launch and operating temperatures. It is desirable to have a compressive prestress in the barrier to minimize tensile stresses produced by launch vibrations. The prestress diminishes during startup, reaching a minimum at the steady-state temperature levels in orbit. The final temperatures are below the softening temperature of the barrier material and well below the range where crystallization takes place.

6. Thermal Stresses in Clad and Barrier at Junction to Upper End Cap

The Hastelloy-N clad and the ceramic barrier are subjected to maximum tensile stresses at the junction of the upper end cap and the clad. These stresses are related to the difference between the average end cap temperature and the adjacent clad temperature. As noted in Section VIII, B, 3b, the maximum temperature difference between the end cap and the clad 0.1 in. away occurs in the

center element and is 49.5°F (Figure 24). The corresponding maximum tensile stresses in the clad and the barrier are 19,710 and 6,570 psi, respectively.

The yield strength of Hastelloy-N is 40,000 psi at 500°F. Consequently, there is an adequate margin of safety for the clad. Because of the bonding procedure used, a residual compressive stress of approximately 25,000 psi exists in the barrier when the element is heated to 400°F during startup. Therefore, the barrier remains in compression throughout the startup sequence.

Another possible source of internal pressure is heating of the helium which is the cover gas used when the fuel element is loaded. However, when the element is sealed, the internal helium pressure is only 250 microns. The partial pressure of helium in the helium-hydrogen mixture is insignificant.

7. Internal Pressure in the Fuel Element

The principal mechanism of pressure buildup inside the fuel element is the dissociation pressure of hydrogen in equilibrium with the monatomic hydrogen of the fuel. Tangential stress in the clad due to dissociation is plotted against temperature in Figure 26 for an N_H of 6.35 and 0.15 w/o carbon. A conservative approach to internal pressure evaluation is to assume that the local pressure exerted on the clad is a function of the local fuel surface temperature (no hydrogen redistribution). With this definition, the lower curve of Figure 26 represents local clad stress vs local clad temperature. Stress rupture data for Hastelloy-N sheet were extrapolated to 10,000 hr and graphed vs temperature in the same figure.

Comparison of the stress level with the ultimate strength of the clad shows that the maximum allowable clad temperature is 1430°F. Maximum expected clad temperature in the SNAP 10A core is 1050°F. Therefore, rupture of the clad due to internal hydrogen pressure is not a limiting consideration for SNAP 10A conditions.

8. Expansion of the Internal Reflectors and Grid Plates

Due to the high thermal conductivity of beryllium and the high heat transfer coefficients in the core, the internal reflectors will operate at temperatures close to those of the adjacent coolant. Axial expansion of the reflector between 70 and 950°F amounts to 0.107 in. compared to the fuel element expansion of 0.075 in.

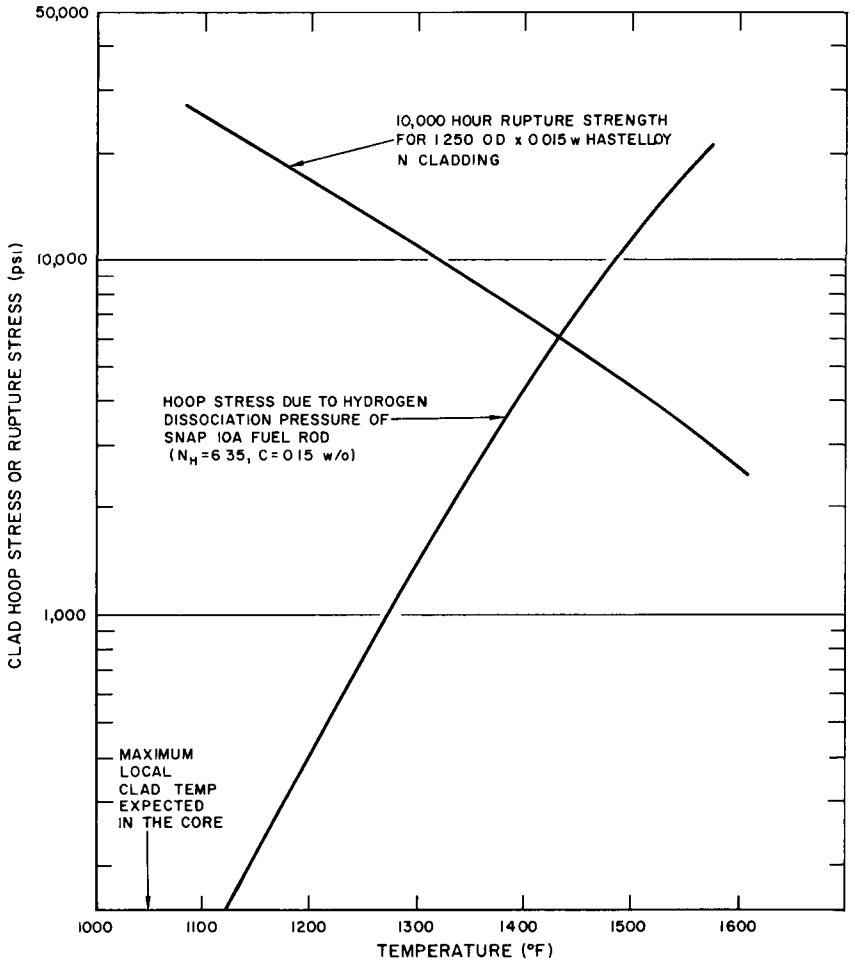

10-4-63 7623-0009

Figure 26. Hoop Stress in the SNAP 10A Reactor Cladding and Long-Term Rupture Data vs Temperature

The lower grid plate, composed of the baffle and orifice plates, will operate at a uniform temperature of approximately 900°F. No thermal stresses will be induced in these plates.

The upper grid plate will have a radial temperature distribution matching the core outlet temperature profile. For an ideally orificed core, the outlet temperatures would be the same for all coolant channels. If a completely uniform velocity profile were to exist, channel outlet temperatures would vary by 80°F, with the center of the plate operating hotter than the periphery. This gradient produces compressive stress on the center of the plate and tensile stresses at the edges, both of which are below 8000 psi. This stress is below yield stress for Hastelloy-C at 1000°F. The plate will not buckle at this stress level.

9. Reactor and Core Pressure Drop

Core pressure drop is made up of a fluid friction loss in the coolant channels plus orifice losses in the openings of the orifice plate and the two support plates. In spite of the fact that the core is orificed, the pressure drop can be fairly approximated by using superficial uniform velocities based on the total flow areas. These velocities and areas are tabulated in Tables IX, X, and XI, along with the calculated pressure drop through each section. Velocities are based on a reactor flow rate of 82 lb/min. Pressure drops are based on a smooth tube friction factor and a pressure loss coefficient of 1.73 for submerged, square-edged orifices.

TABLE IX

CALCULATED SNAP 10A PRESSURE DROP USING SUPERFICIAL UNIFORM VELOCITIES BASED ON TOTAL FLOW AREA

	Flow Area ($in.^2$)	Velocity (ft/sec)	Pressure Drop (psi)
Reactor Inlet Nozzle (2)	1.29	3.22	0.054
Baffle Plates (2)	7.96	0.69	0.005
Orifice Plate	2.60	1.60	0.023
Coolant Channels	6.00	0.70	0.010
Reactor Outlet Nozzle	1.11	3.82	0.078
Total for Reactor			0.170

Reactor entrance and exit losses were based on 1.0 and 0.23 velocity head losses for sudden expansion and contraction, respectively. Since these two losses make up 78% of the total pressure drop, accuracy in the total figure must suffer due to inexact knowledge of entry and exit coefficients.

TABLE X

SNAP 10A CORE PARAMETERS DURING ACTIVE CONTROL

Total reactor power (kw)	34.7
Reactor heat to NaK (kw)	34.2
Heat loss from vessel at operating temperatures (kw)	0.50
Core radial peak/average power factor	1.47
Core axial peak/average power factor	1.31
Fuel element peaking factor	1.00
Design NaK flow rate (lb/hr)	4920
Flow areas	
Area of 54 tri-cusp channels ($in.^2$)	3.987
Area of 18 side channels ($in.^2$)	1.118
Area of 12 unorificed peripheral channels ($in.^2$)	0.935
Total core flow area	6.04
Area of openings in orifice plate ($in.^2$)	2.60
Area of openings in baffle plates ($in.^2$)	7.96
Equivalent diameters	
Tri-cusp channels (in.)	0.151
Side channels (in.)	0.075
Core average (in.)	0.123
Number of fuel elements	37
Number of internal reflectors	6
Total active heat transfer area in core (ft^2)	12.35
Heat transfer coefficient at surface of center fuel element ($Btu/hr\text{-}ft^2\text{-}°F$)	1860
Reactor inlet temperature (°F)*	900
Reactor outlet temperature (°F)*	1010

*Nominal values during active control period

TABLE XI

CORE MATERIALS AND PHYSICAL PROPERTIES AT 950°F

	Material	Density (lb/ft^3)	Specific Heat (Btu/lb-°F)	Conductivity ($Btu/hr-ft^2-°F$)
Internal Reflectors	Be	113	0.65	76
Grid Plates	Hastelloy-C	558	0.09	5.
Fuel	ZrH+10 wt% U	350	0.15	13
Fuel Element Cladding	Hastelloy-N	538	0.10	10.9
Diffusion Barrier	-	140	0.20	1
Coolant	NaK-78	46.8	0.209	15
Gas Gap	H_2			0.20
Nominal core pressure (psia)				5
Minimum core pressure (psia)				2
Maximum core pressure (psia)				10
Calculated reactor pressure drop (psia)				0.17
Vapor pressure of NaK at 1000°F (psia)				0.8
Vapor pressure of NaK at 1100°F (psia)				1.7
Maximum clad surface temperature (°F)				1050
Maximum fuel temperature (°F)				1085

Core Dimensions	
Fuel element pitch (triangular arrangement)	1.260 ± 0.003
Fuel element diameter (cladding OD)	1.250 ± 0.002
Clad thickness	0.015 ± 0.0005
Fuel length	12.25 ± 0.002
Diffusion barrier thickness	0.0025 ± 0.0020
Diametric fuel-clad clearance	0.005 ± 0.0015
Fuel diameter	1.2100 ± 0.0005
ID of coated cladding	1.215 ± 0.001

BLANK

IX. REENTRY BEHAVIOR

The discussion which follows is restricted to reentry of the SNAP 10A-Agena satellite from orbit. Reentry as a result of failure during the ballistic launch trajectory is not considered herein.

The reentry configuration of the SNAP 10A-Agena, which enters the sensible atmosphere at 400,000 ft after orbital decay is shown in Figure 27. The vehicle velocity vector passes through the vehicle center of mass, and lies below the local horizon. The local horizon is tangent to the atmospheric surface or perpendicular to the radius vector to the center of the earth. Local horizon, flight angle, and a scale earth-atmosphere-orbit relationship are shown by the figure.

Only that portion of the atmosphere below 400,000 ft is important to reentry heating breakup. The actual atmosphere of the earth is a thin shell wrapped on an oblate spheroid. Considering the SNAP 10A polar orbit, it has been shown that the vehicle orbit can never give constant altitude for all latitudes. Thus, an initial altitude over the pole does not correspond to the same phase of orbit decay as does the same altitude over the equator. This effect will not significantly affect the degree of reactor heating and ablation.

Mission requirements require that the SNAP 10A-Agena make one revolution per orbit resulting in the reactor always facing outward from earth. Therefore, the vehicle will enter the atmosphere with some angle of attack with an angular rate. This event is shown in Figure 28 for the nose forward aerodynamic configuration of the SNAP 10A- Agena. The resultant of the aerodynamic forces shown by Figure 28 acts through the vehicle center of pressure imposing a moment, forcing the vehicle towards zero angle of attack. The vehicle will oscillate about the center of gravity with the reactor orientated forward due to aerodynamic stability. The SNAP 10A power system achieves aerodynamic stability in the same manner as does the SNAP 10A-Agena vehicle as shown in Figure 28. The SNAP 10A reactor has neutral aerodynamic stability, and has a tumbling entry mode since there are no restoring aerodynamic forces acting away from the center of mass.

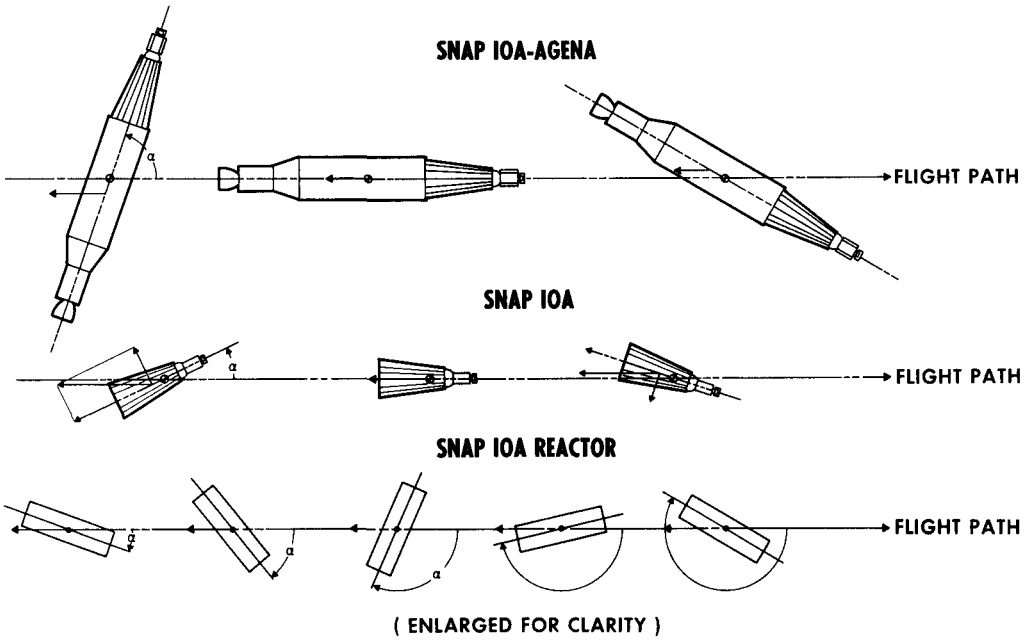

5-2-63 7573-1071-A

Figure 27. SNAP 10A Reentry Configuration Sequence

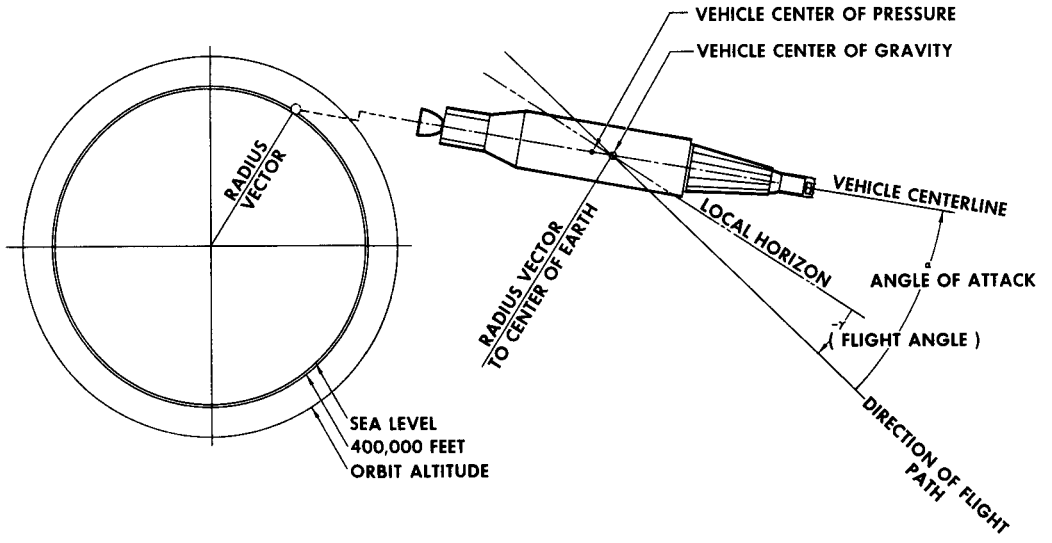

5-2-63 7573-1068

Figure 28. SNAP 10A Typical Polar Orbit and Vehicle Configuration

The initial point in the orbital decay calculations was taken at 400,000 ft over the North Pole. Trajectory calculations were accomplished with the RESTORE Code for the respective ballistic parameters dependent upon aerodynamic mode, free molecular or continuum, and particular component weight. The reentry trajectories are shown in Figure 29.

The probability of a NaK filled system depends on orbit lifetime. However, the combination of surface coatings on the vessel and reflectors assures that, if NaK is present in the reactor, the NaK will be in a liquid state when reentry commences. The reentry events for both a system devoid of NaK and a NaK filled system are described in the following paragraphs.

A. REENTRY OF A SYSTEM DEVOID OF NaK

The SNAP 10A reentry trajectory is shown in Figure 29 where flow transition and major separation sequences are indicated. Satisfaction of relating reentry burnup to altitude requires that the heating functions to individual vehicle components be known during the reentry sequence. The oscillation envelope for the SNAP 10A-Agena was calculated with a two-dimensional oscillation code that related vehicle moment of inertia, and aerodynamic restoring moment into angular rates. The oscillation envelope and dynamic pressure for this reentry case are shown in Figure 30, where the effect of increasing dynamic pressure results in a reduced oscillation amplitude and increase in frequency. Knowlege of the vehicle velocity and attitude then provides criteria for calculation of heating rates. The spherical stagnation heating rate and vehicle velocity are presented in Figure 31 for reference.

1. Reflector Retainer Band-Reflector Ejection

Heating of the reflector retainer band becomes appreciable above 300,000 ft. The oscillation entry mode of the vehicle will result in an oscillating transient temperature on any particular band segment. This oscillating temperature is the result of the aerodynamic heating being applied to a variable projected band surface area and cyclic reactor shadow on the band. The retainer band, not considering fusible links, will have cycled through the melting temperature of stainless steel by an altitude of 285,000 ft. When the band parts, the reflectors fall away. They are retained only by the cable harness containing electrical connections to the actuator motors and reflector instrumentation. Once ejected,

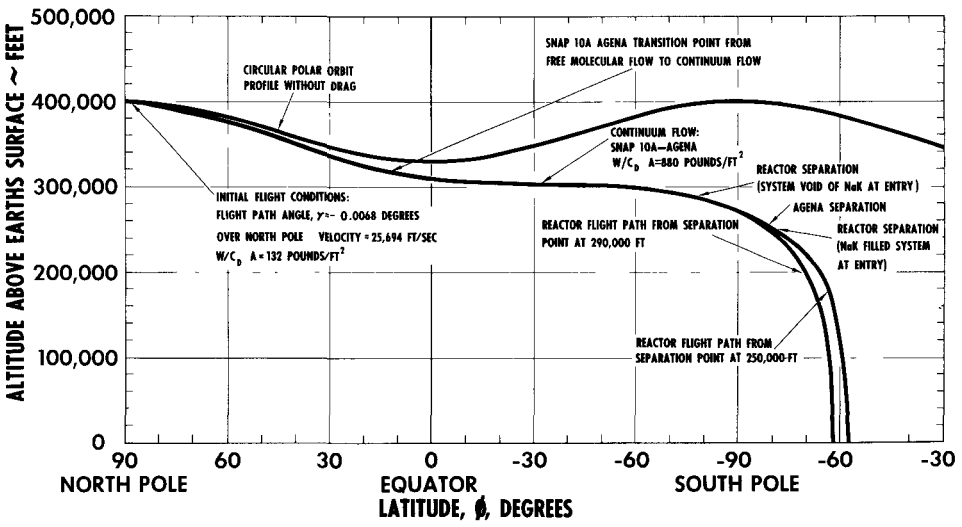

5-2-63 7573-1072B

Figure 29. SNAP 10A Reentry Trajectories

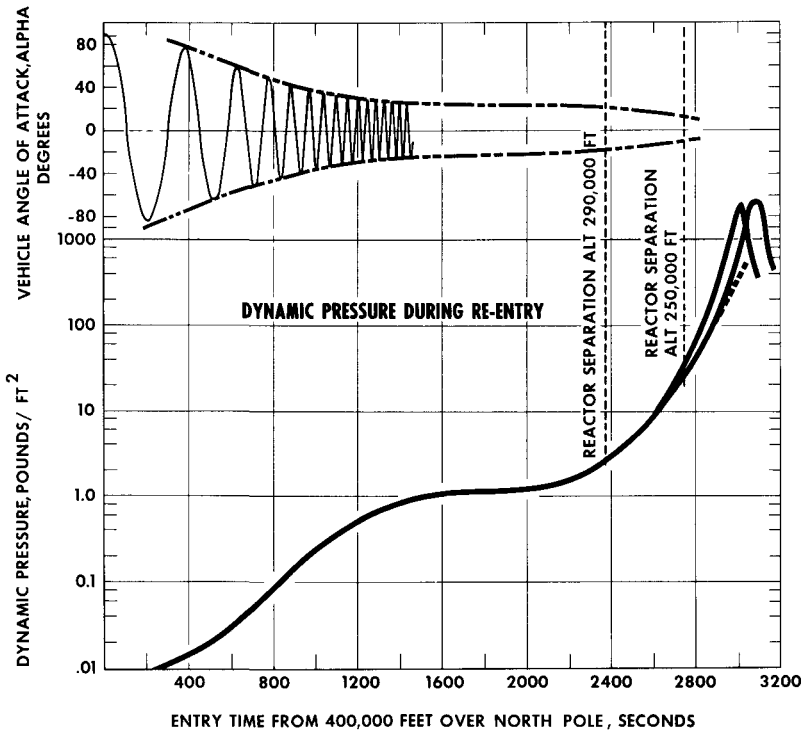

5-2-63 7573-1066a

Figure 30. SNAP 10A Oscillation Envelope and Dynamic Pressure During Reentry

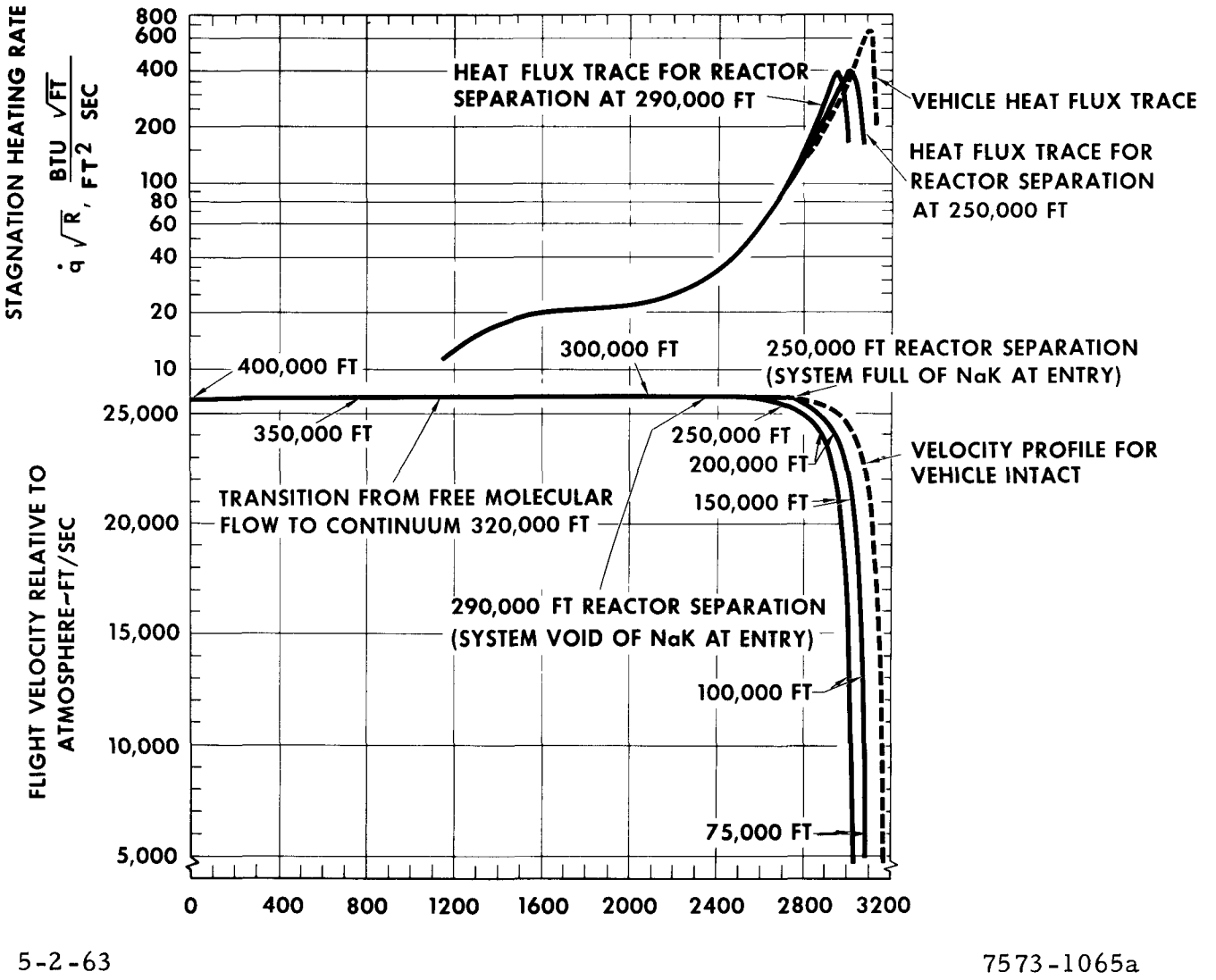

5-2-63

7573-1065a

Figure 31. Continuum Regime Heating Rate and Flight Velocity Profile

the reflectors will pivot until they contact the reactor support legs and the tip of the shield. In this position, the cable harness is exposed to aerodynamic heating and the pull of aerodynamic drag acting on the large exposed surfaces of the reflector. Complete release of the reflectors is expected above 280,000 ft.

2. Thermoelectric Pump

The aluminum radiators of the thermoelectric pump will be completely ablated by 280,000 ft. The primary effect of this event is to increase the aerodynamic heating on the upper surface of the reactor vessel. The top surfaces of the magnets will have started to ablate by this altitude. However, the reactor vessel top will separate prior to complete magnet ablation. The transient temperature rise of the aluminum radiator fins are presented in Figure 32. The temperature of the fins rises at a slow rate due to high emissivity coating which reradiates heat to space.

3. Reactor Separation

Reactor separation depends on ablation of the four titanium support legs, NaK inlet, and outlet pipes. The forward portion of the NaK outlet pipe will receive the greatest heating rate of these components during reentry and will burn through at 295,000 ft. The reactor is then attached to the converter structure via four titanium support legs which follow the outline of the top of the shield. The 0.032-in.-thick titanium wall will readily melt exposing the portion of the stainless steel NaK lines where the walls are 0.020-in. thick. The ablation of the reactor inlet NaK lines is complete by 290,000 ft. At this point, the reactor will separate from the converter structure and begin to tumble. The reactor will continue toward earth on a trajectory dependent upon a ballastic parameter made up from the reactor weight, projected area to the air stream, and the drag coefficient of a tumbling cylinder.

4. Agena Separation

The converter structure-Agena complex remains aerodynamically stable after reactor separation and continues reentry in an oscillating mode nose forward. The aerodynamic heating rate continues to increase after reactor separation, as shown by Figure 31, resulting in burning away of the converter structure and severe heating at the SNAP 10A-Agena connector ring. The structure of the connector will fail by 250,000 ft providing breakup of the vehicle into segments of questionable aerodynamic stability.

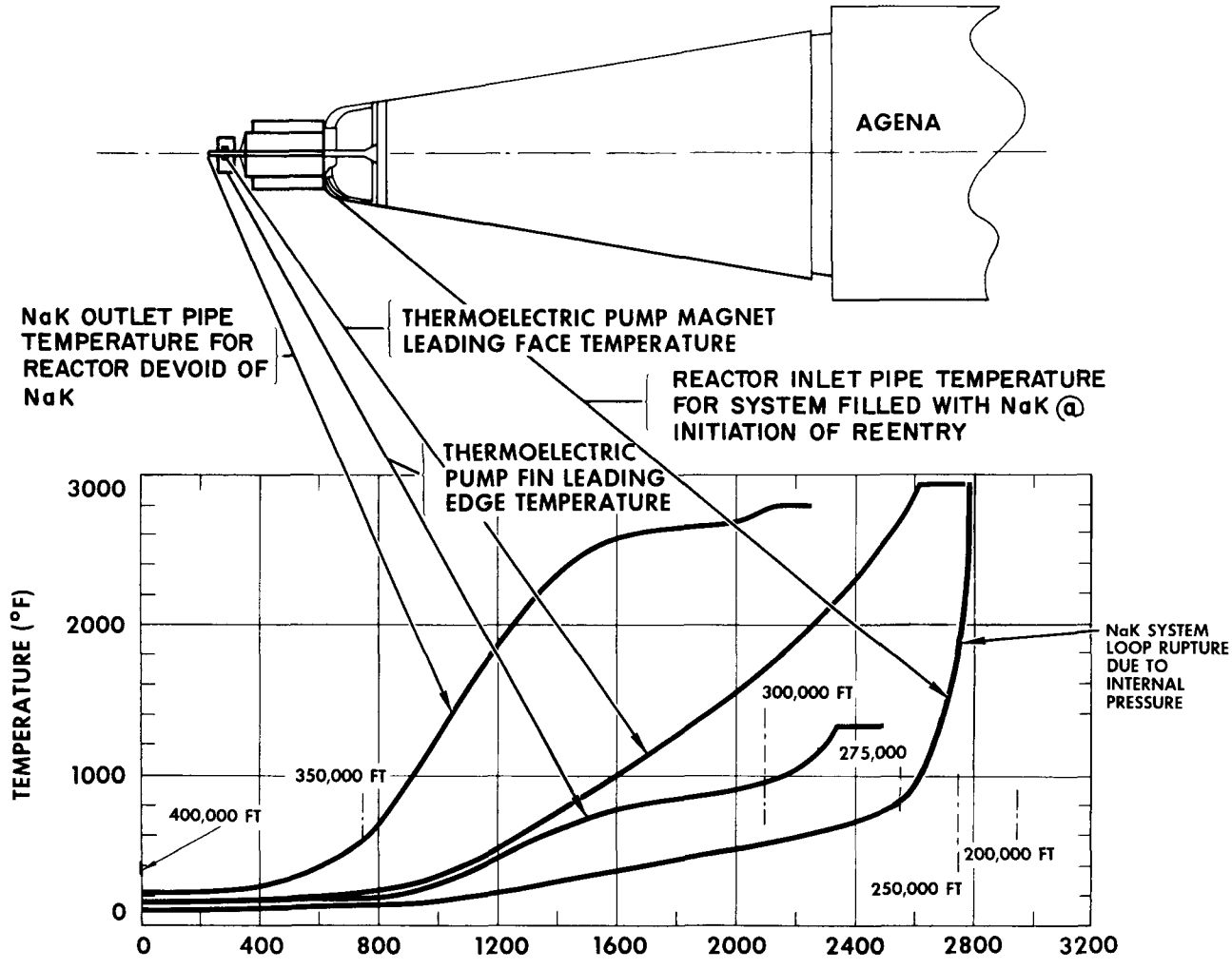

5-2-63 7573-1067B

Figure 32. Temperature Profiles During S10A Reentry

B. NaK FILLED SYSTEM AT ENTRY

The presence of NaK in the SNAP 10A system will retard reentry ablation by absorbing a portion of the available aerodynamic heat production. A conservative analysis must therefore be based on a NaK system which has not been penetrated prior to reentry and has a flow rate, probably in the reverse direction of operation, due to the aerodynamic heating of the thermoelectric pump radiator fins.

The NaK system will be simultaneously heated at four principal points: (1) the reactor outlet lines at the forward end of the power unit normal to the flight path, (2) the reactor outlet lines where they penetrate the vessel support legs, (3) the converter tubes, (4) the upper converter manifold. Heating is greatest where the lines are aligned normal to the air stream; the first penetration will be made at the outlet lines ahead of the reactor. The entire reactor system will heat up as a result of NaK circulation transmitting the heat from local hot points where aerodynamic heating supplies energy to the system. The average temperature of the system where NaK is flowing is shown in Figure 32.

1. Reflector Retainer Band-Reflector Ejection

The NaK in the system has no effect on the retainer band, and reflector ejection will occur above 280,000 ft as given for the system entering devoid of NaK.

2. Reactor Separation

The event of reactor separation is delayed due to the removal by the flowing NaK of the necessary energy to raise the NaK inlet and outlet pipes to their melting temperatures. The four titanium support legs will melt away exposing the NaK inlet lines to the airstream, thus resulting in NaK line ablation when the NaK system ruptures. Separation of the reactor is expected to occur by 250,000 ft due to inlet and outlet NaK pipe burn-through. Complete ablation of the thermoelectric pump fins, degradation of the pump thermoelectrics, and loss of magnetism by 280,000 ft will result in termination of NaK flow. The

temperature of the NaK lines exposed to aerodynamic heating will rise sharply since heat will no longer be carried away in quantity by the flowing NaK. The most probable point of first penetration will be the forward NaK lines due to the magnitude of the aerodynamic heating at this location. However, system rupture is assured by failure of the expansion compensator at a pressure between 100-200 psi (1900-2200°F). NaK system rupture, followed by NaK line burn-through and reactor separation will occur above 250,000 ft.

C. REACTOR VESSEL ABLATION

The free tumbling reactor vessel trajectories begin at 290,000 ft and 250,000 ft for the respective systems where NaK is absent or contained at entry. These trajectories are shown in Figure 29.

The heating of the reactor vessel during the tumbling mode will be greatest at the upper and lower circumferences of the vessel. Since the lip weld on the vessel head has been exposed to aerodynamic heating from the beginning of reentry, it should be the first part of the vessel to experience complete peripheral melting. The reactor vessel and grid plates ablate by 220,000 ft in both cases, with and without NaK in the core. This result is due to the respective energy (temperature) levels of the reactors at separation. The reactor separated at 290,000 ft has a comparatively cool interior, on the order of 200°F, while the reactor separated at 250,000 ft has been heated in excess of 1200°F due to NaK circulation.

The cluster of rods that becomes exposed to the air stream above 220,000 ft will probably separate into individual fuel elements, but there is a possibility that the cluster of fuel rods may be fused together. If the fuel rods separate it is highly probable that the individual fuel elements will burn up from this altitude.

If the fuel rods remain in a cluster of 37 rods they will not ablate an appreciable amount. However, the temperature of 60% of the fuel rod volume will exceed 2100°F during this last phase of reentry expelling the hydrogen from this volume.

BLANK

X. STEADY-STATE OPERATION OF A SNAP 10A REACTOR IN A RAIN-FILLING CRATER

If the SNAP 10A reactor core should survive the aerodynamic heating and impact reentry forces and remains in a configuration capable of criticality, the possibility of quasi-steady-state reactor operation exists under certain environmental conditions. Since a water impact, in this case, would almost certainly lead to a power excursion which would in turn destroy the reactor, only land impacts need to be considered. Further, if the reactor survives the impact forces, some penetration of earth is probable, possibly leaving the reactor resting in a small crater. Under these conditions, it is possible that water could collect around the reactor to a sufficient degree for criticality to be regained. If the water input (most likely through rainfall) is of the proper rate, steady-state operation of the reactor can occur.

An approximate relationship between reactivity insertion rate and rain rate may be developed for a specified crater size. An upper limit on rain rate for the approach to steady-state operation may then be set by consideration of the maximum reactivity insertion rate which would not cause fuel damage during the initial power pulse.

The rain rate may also be related to the steady-state power of the reactor. Under the condition that heat losses other than for boiling off of water are negligible, the steady-state reactor power must be equivalent to the water boil-off rate. The steady-state power level is limited to a value below which the corresponding temperature and hydrogen diffusion will not cause cladding rupture. Hence, a second relationship limiting the rain rate for steady-state operation in various size craters may be obtained. The subsequent discussion assumes: (1) the reactor core of radius R_1 is resting on end in center of cylindrical crater with radius R_2; (2) the core vessel is open at both ends, and (3) water flows into the core bottom from the filling crater (i.e., the impact has not plugged the coolant flow passages). This situation is illustrated in Figure 33.

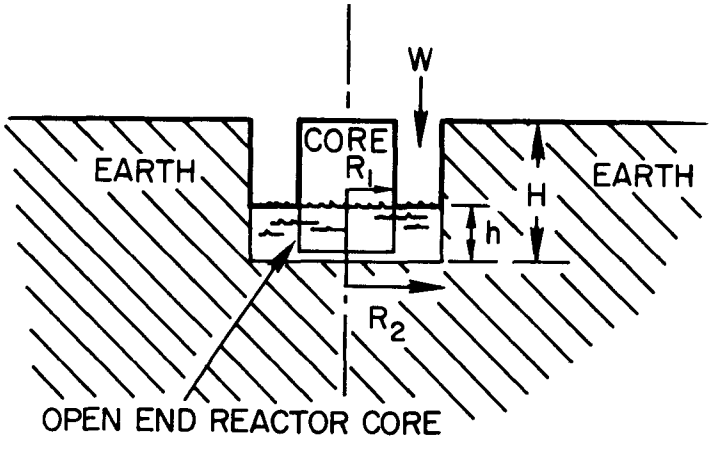

7-10-63 7623-0007

Figure 33. Core in Center of Cylindrical Crater During Rainstorm

In Figure 34, curves are displayed which represent the steady-state rain rates as a function of crater size for particular steady-state power levels. The maximum power possible without rod damage has been estimated at 130 kw.[12] The basis of this estimate was that rod damage would occur at temperatures of 1600°F or over. Therefore steady-state operation certainly must lie below the 130-kw line.

In all probability the reactor, after impacting on soil, will be plugged with dirt at one end of the core. For this case the maximum power which can be generated in the core is 6 kw[12] before rupture of the fuel element occurs due to overheating. Consequently, it is highly improbable that steady-state operation will occur above the 5 kw curve shown in Figure 34.

The upper curve in Figure 34 represents the maximum rain rate below which the rods will not be damaged as a result of the initial power pulse associated with the rising water level. This curve was obtained using 2¢/sec as the maximum allowable reactivity insertion rate. The value of the rain rate must lie beneath these two curves for possible steady-state power operation. It has been estimated that the reactor cannot achieve criticality for (R_1/R_2) ratios larger than 0.7 even with water surrounding the height of the core. For this reason steady-state operation must lie to the left of the vertical line drawn in at $R_1/R_2 = 0.7$.

The top curve of Figure 35 represents the steady-state power associated with the maximum rain rate which would not cause rod damage on the first power pulse. The other curves on Figure 35 represent steady-state power levels associated with rain rates from 2.5 to 10 in./hr. If an upper limit could be set for rain rate and a lower limit could be set for the ratio R_1/R_2 the possible steady-state operation range would be limited accordingly. For example, assume that the crater formed is five times larger in radius than the reactor core. Further, assume that it is improbable to have rain rates exceeding say, 2-1/2 in./hr. Examination of Figure 35 would then lead to the conclusion that steady-state power operation at levels exceeding 45 kw would be very improbable.

Use has been made of a reactivity per inch change in water level rate applicable to the case of water levels about the center few inches of core height. This use is justified in the case of small (R_1/R_2) ratios in that the reactor core can go cold-critical when the water level reaches 6.45 in. As (R_2-R_1) decreases below 4 in. the reflector no longer appears infinite and criticality would occur for higher water levels with a corresponding decrease in reactivity worth per unit change in water level.

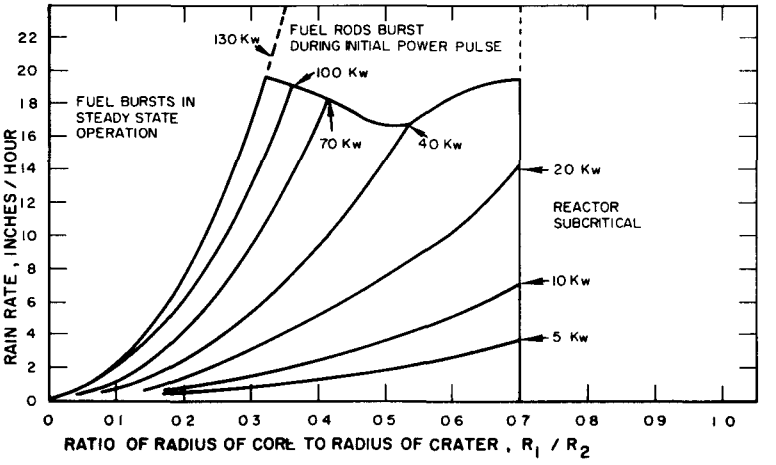

7-10-63 7623-0005

Figure 34. Variation of Rain Rate with Crater Size for Various Steady-State Power Levels

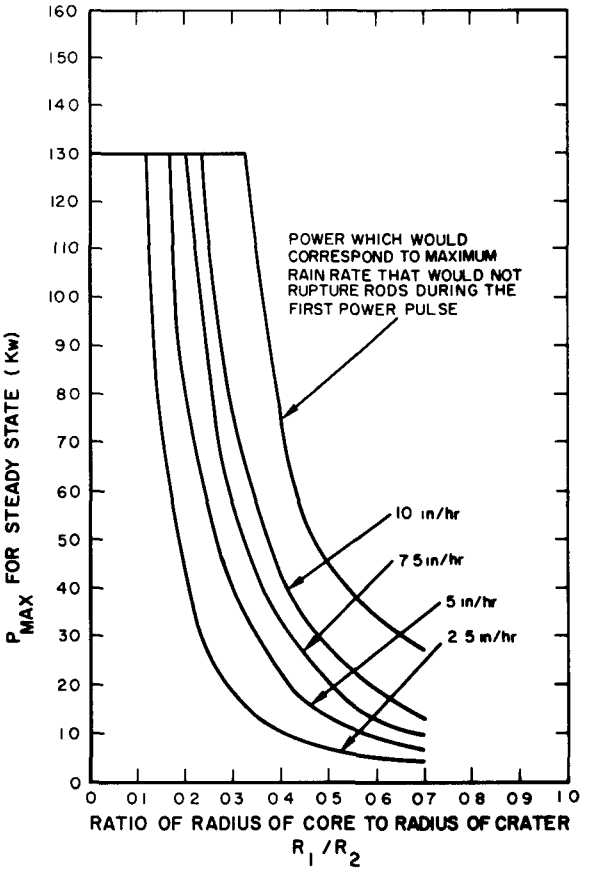

7-10-63 7623-0006

Figure 35. Maximum Steady-State Power for Various Rain Rates and Crater Sizes

BLANK

XI. STEADY-STATE OPERATION OF A SNAP REACTOR IN A SPACE ENVIRONMENT

Failure of the band release devices could result in continuous reactor operation in orbit. If the reactor is not shut down by reflector ejection, power will gradually decay due to fuel depletion, fission product buildup, and hydrogen leakage. Since power decay and declining temperatures will diminish the rate of burnup and hydrogen loss, operation in the power range can continue almost indefinitely. The present study of long-term reactor operation has been based on failure of the coolant circulation system with the expectation that loss-of-flow or loss-of-coolant will occur within a decade following launch. Nearly every mode of system failure can be categorized as leading to one of two modes of circulation system failure. Some of the causes of system failure are:

1. Thermal and electrical degradation of the pump thermoelectric materials
2. Nuclear radiation damage to the pump thermoelectrics
3. A high resistance film built up on the pump throat due to contamination of the NaK
4. A breakdown of the high emissivity coating on the pump radiators
5. A loss of the bond between the thermoelectrics and the radiators in the pump
6. A loss of the bonds in the thermoelectric elements of the converter
7. A meteoroid puncture of the NaK line
8. Erosion of the NaK line walls or connections.

Items 1 through 5 will cause NaK stagnation in the core. Item 6 produces stagnation as a secondary effect by increasing the rate of thermal degradation of the NaK pump. Items 7 and 8 will cause a loss of NaK from the system. In addition to the causes listed above, it is possible that NaK boiling can occur resulting in excessive pressures and temperatures causing loss of NaK through failure of NaK system components (e. g., expansion compensators) or failure of the fuel elements.

The immediate effect of coolant system failure is an increase in all temperatures in the core and decrease in power due to negative fuel and grid plate temperature coefficients. An equilibrium is obtained at a power level of a few hundred

watts with heat being rejected directly from the thermally-isolated reactor vessel.

After the initial loss-of-flow or loss-of-coolant transient, burnup of the fuel and hydrogen loss would result in the reduction of the reactor power level as shown in Figure 36. Two conditions of power removal corresponding to radiation to dark sky and radiation in full sun are also shown in Figure 36. The exact case for the particular orbit under consideration will be enclosed within these two extremes. After about 2000 years the system power level will be reduced to about 28 to 48 watts for full sun conditions and 90 to 250 watts for dark sky conditions.

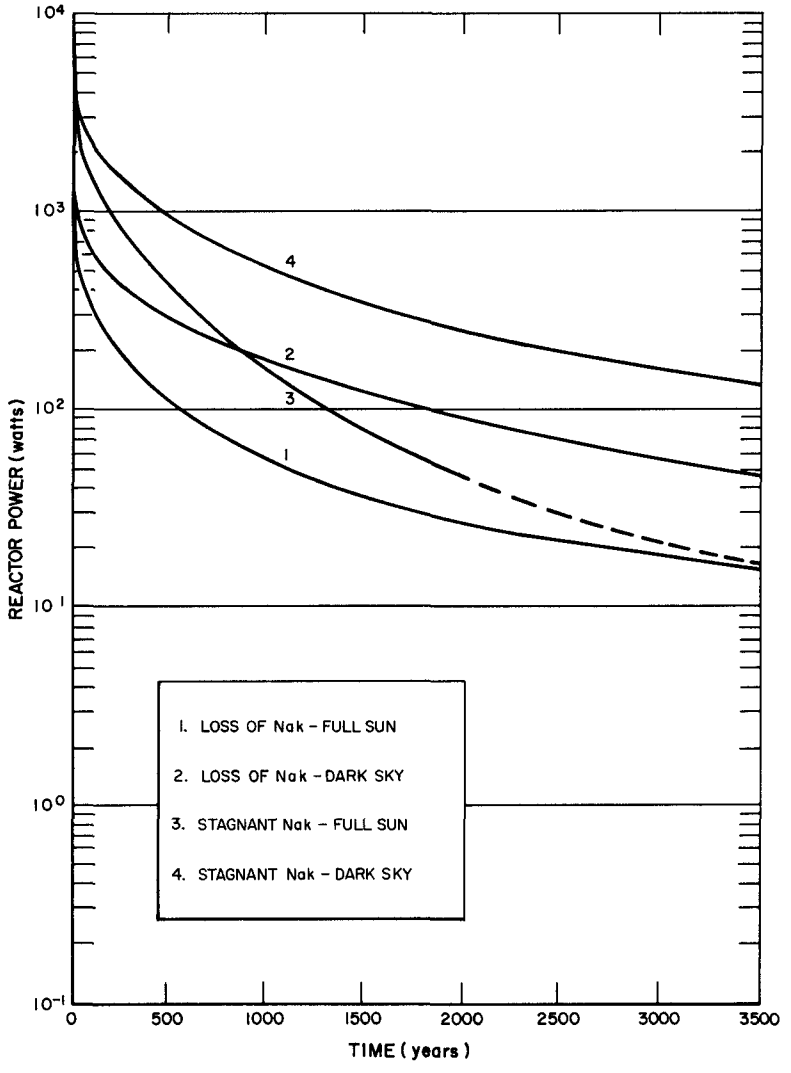

7-10-63 7623-0001

Figure 36. SNAP 10A Reactor Power Decay

REFERENCES

1. Thiele, A. W. and C. A. Guderjahn, "SNAP 2 Hydride-Moderated Critical Assembly," NAA-SR-3620 (1959) SECRET

2. Wilson, L. A., "SNAP 2 Experimental Reactor Physics Analysis," NAA-SR-3607 (1959) SECRET

3. Clark, F. H., et al, "Analysis of S2DR Design," NAA-SR-5890 (1961)

4. Flatt, H. P. and D. C. Baller, "The AIM-6 Code," NAA-SR-4694 Addendum (1960)

5. Stone, S., "ZOOM, A One-Dimensional Multi-Region, Multi-Group Diffusion Code for the 704," U. C. R. L. 5293 (1960)

6. Wachspress, E. L., "A Generalized Two-Space Dimension Multigroup Code for the IBM-704," KAPL-1724 (1957)

7. Vargofcak, D. S., "ULCER," NAA Program Description AMTD-123 (1962)

8. Lemke, Barbara, "FORTRAN SNG Code," NAA Program Description (1959)

9. Rooney, K. L., "FARSE-1A, A Modification of FARSE to Include Angular Dependence of Shield Leakage," TDR 5954 (1960)

10. Goetz, C. A., "SCAR-1, Scattered Fast Neutron Current From an Ion Motor Ring," NAA-SR-6191 (1961)

11. General Electric Aircraft Nuclear Propulsion Department, "Shielding Computer Program 14-0 and 14-1 Reactor Shield Analysis," XDC59-2-16 (1959)

12. Mims, L. S., "Analysis of SNAP 10A Reactor Immersed in Slowly Rising Water," NAA-SR-MEMO-8271 (1963)